

Large-amplitude high-frequency waves at Earth's magnetopause

D. B. Graham, +IRFU, +MMS

[Graham, D. B., Vaivads, A., Khotyaintsev, Yu. V., Andre, M., et al. (2018). Large-amplitude high-frequency waves at Earth's magnetopause. *Journal of Geophysical Research: Space Physics*, 123.<https://doi.org/10.1002/2017JA025034>]



Outline

- Background and motivation
- Theory
- Wave observations
- Statistical results
- Conclusions

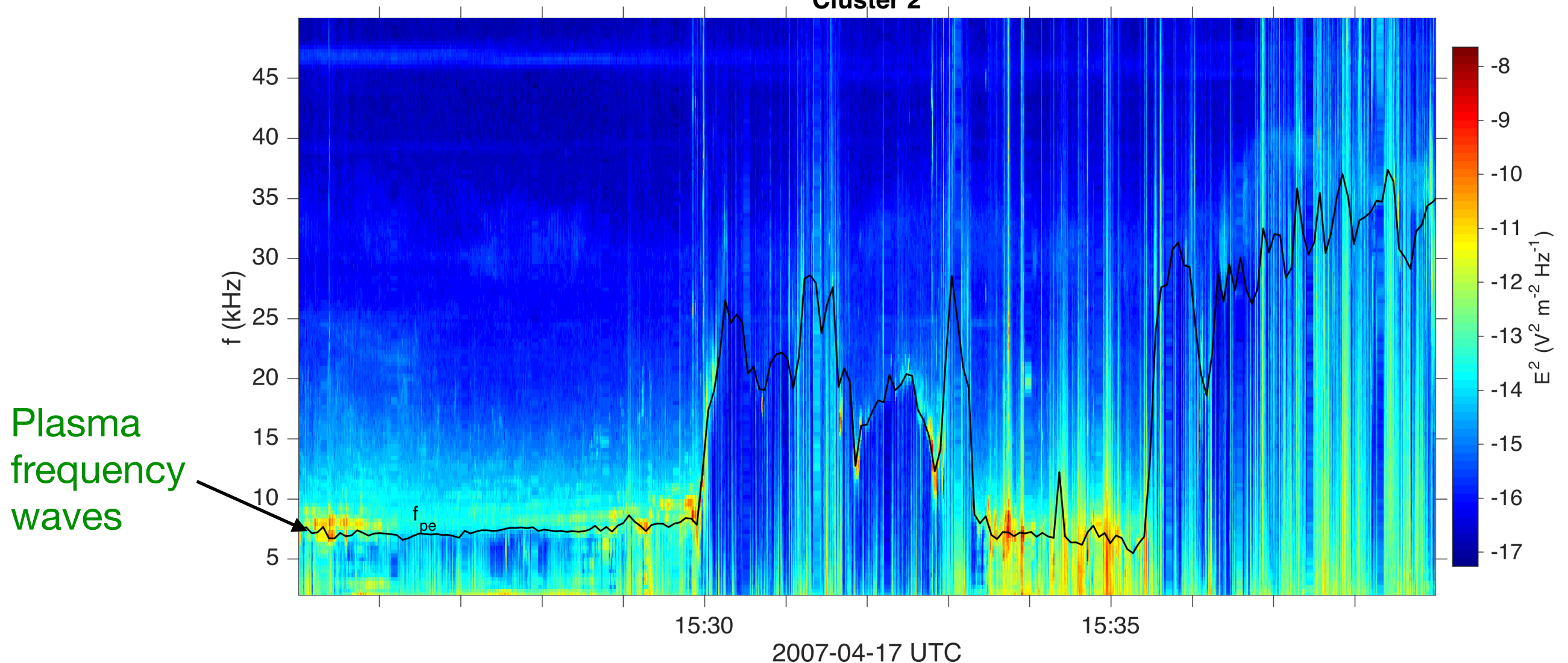
Background and motivation

- Langmuir ($k_{\parallel} \gg k_{\perp}$) and/or upper hybrid ($k_{\parallel} \ll k_{\perp}$) waves have been reported at Earth's magnetopause.

[e.g., Gurnett et al., 1978;
Anderson et al., 1982]

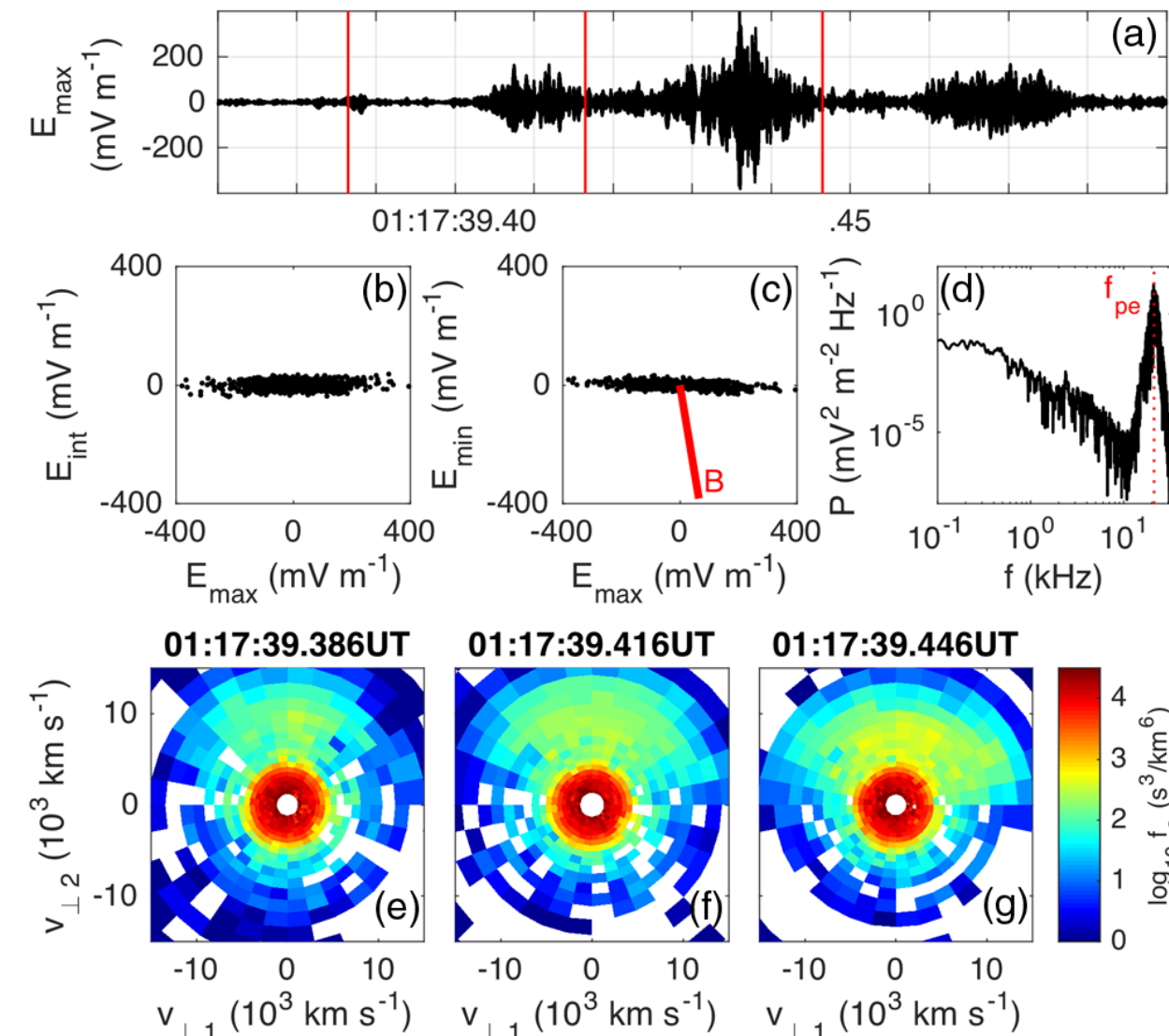
Waves at the magnetopause

Cluster 2



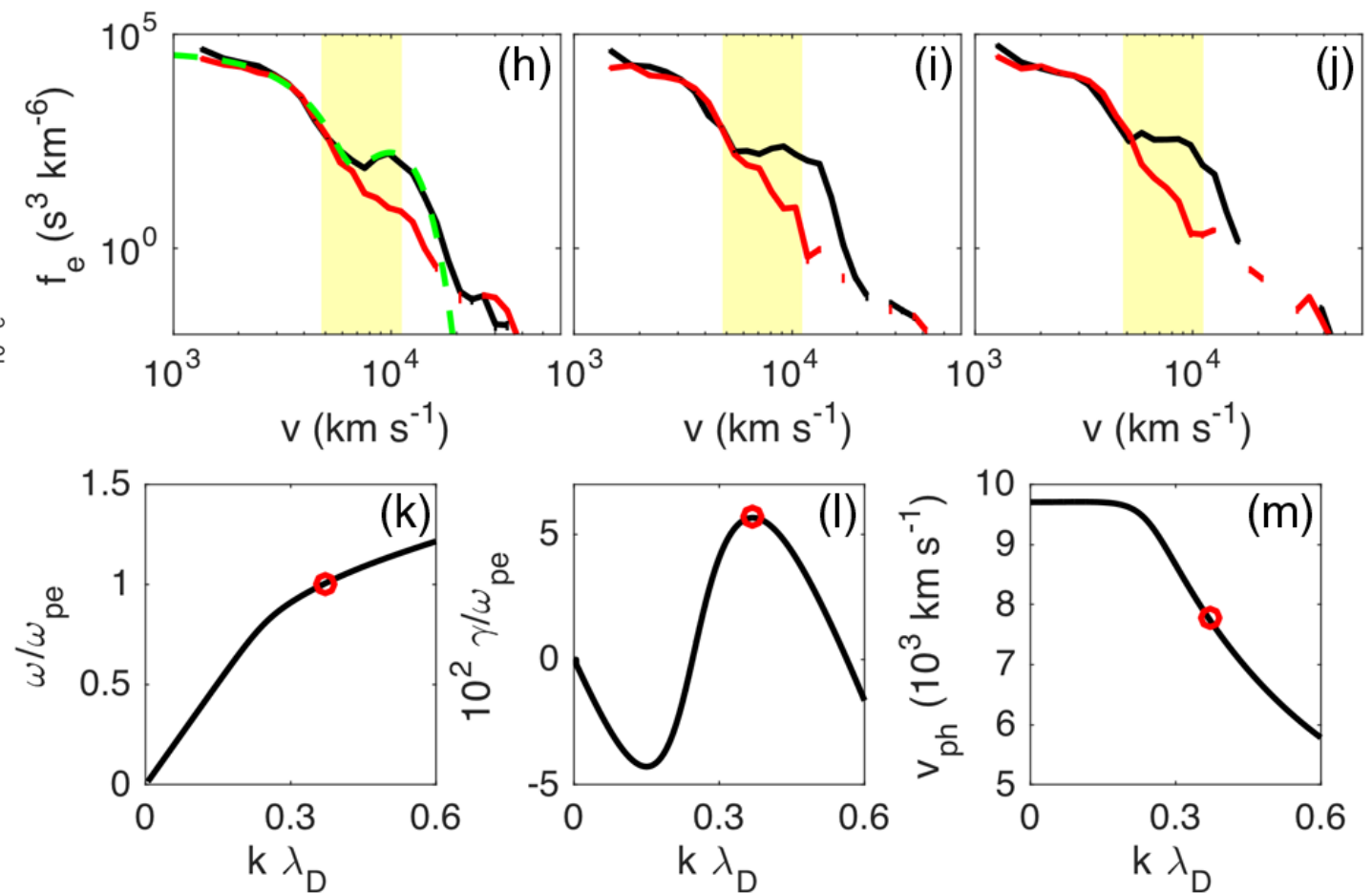
Magnetic reconnection

- Plasma frequency waves generated near a reconnection electron diffusion region.

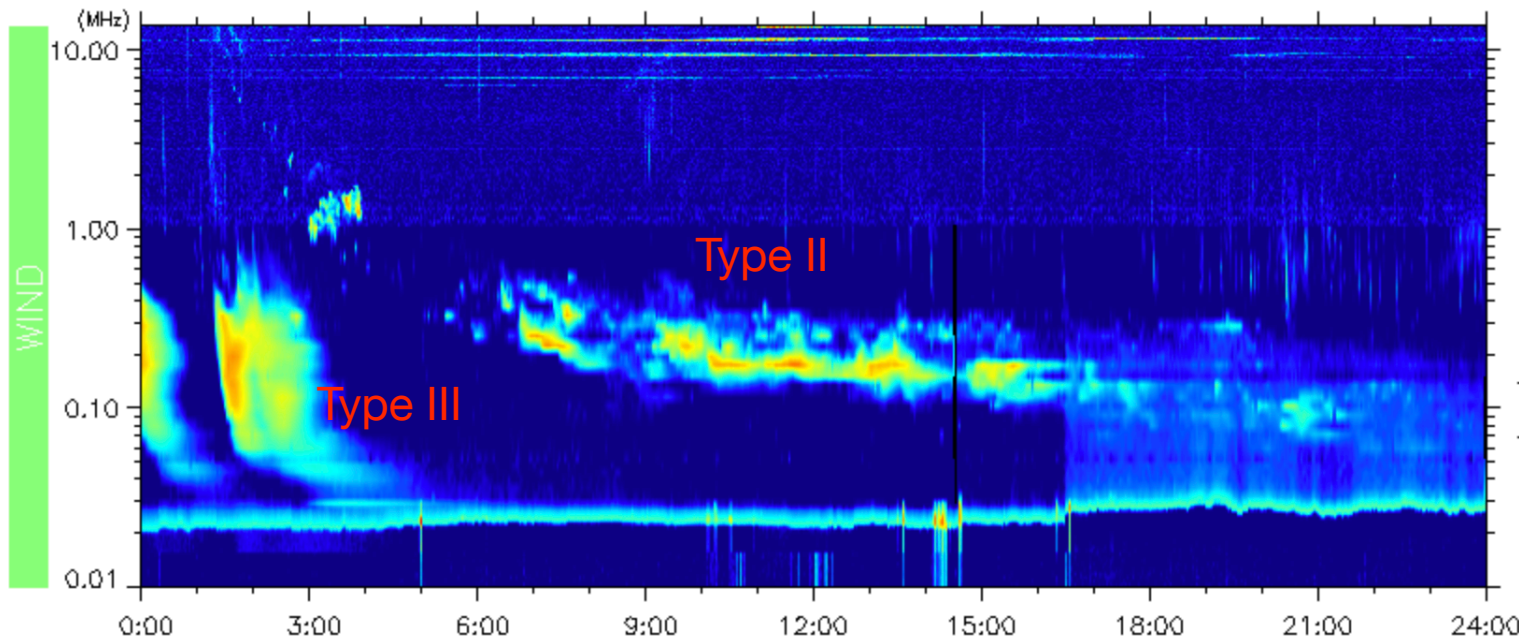


- Waves are generated by an agyrotropic electron beam.

[Graham et al., 2017]



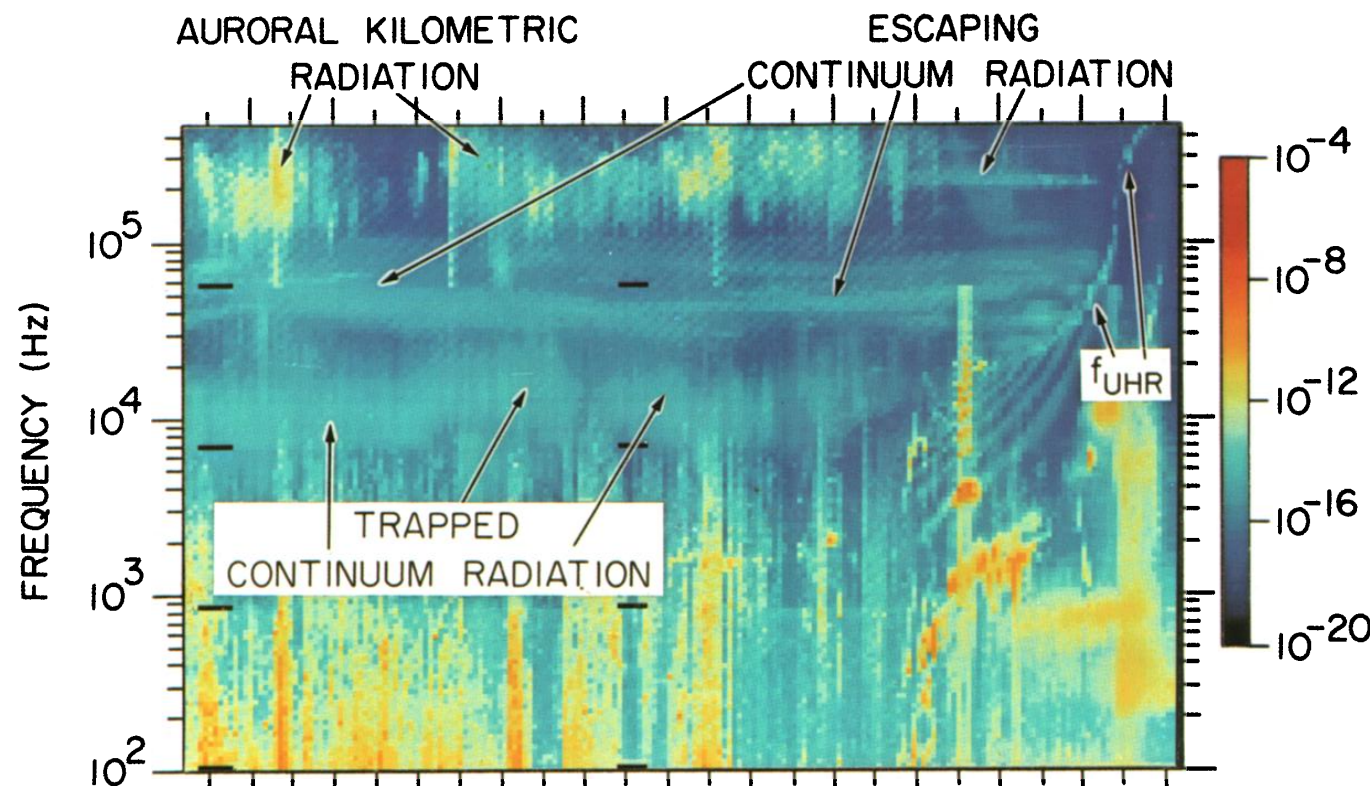
Radio emission



- Type II and type III radio bursts (Wind data).

2017 July 14

DAY 95, APRIL 5, 1978



- Langmuir and UH waves can generate radio waves by linear or nonlinear processes.

- Continuum radio emission and AKR.

UT	0200	0400	0600	0800	1000	1200										
λ_m (DEG)	14.2	16.3	15.4	11.0	3.0	-12.1										
MLT (HR)	1.1	1.2	1.3	1.5	2.0	3.5										
R (R_E)	17	16	15	14	13	12	11	10	9	8	7	6	5	4	3	2

[Kurth et al., 1981]

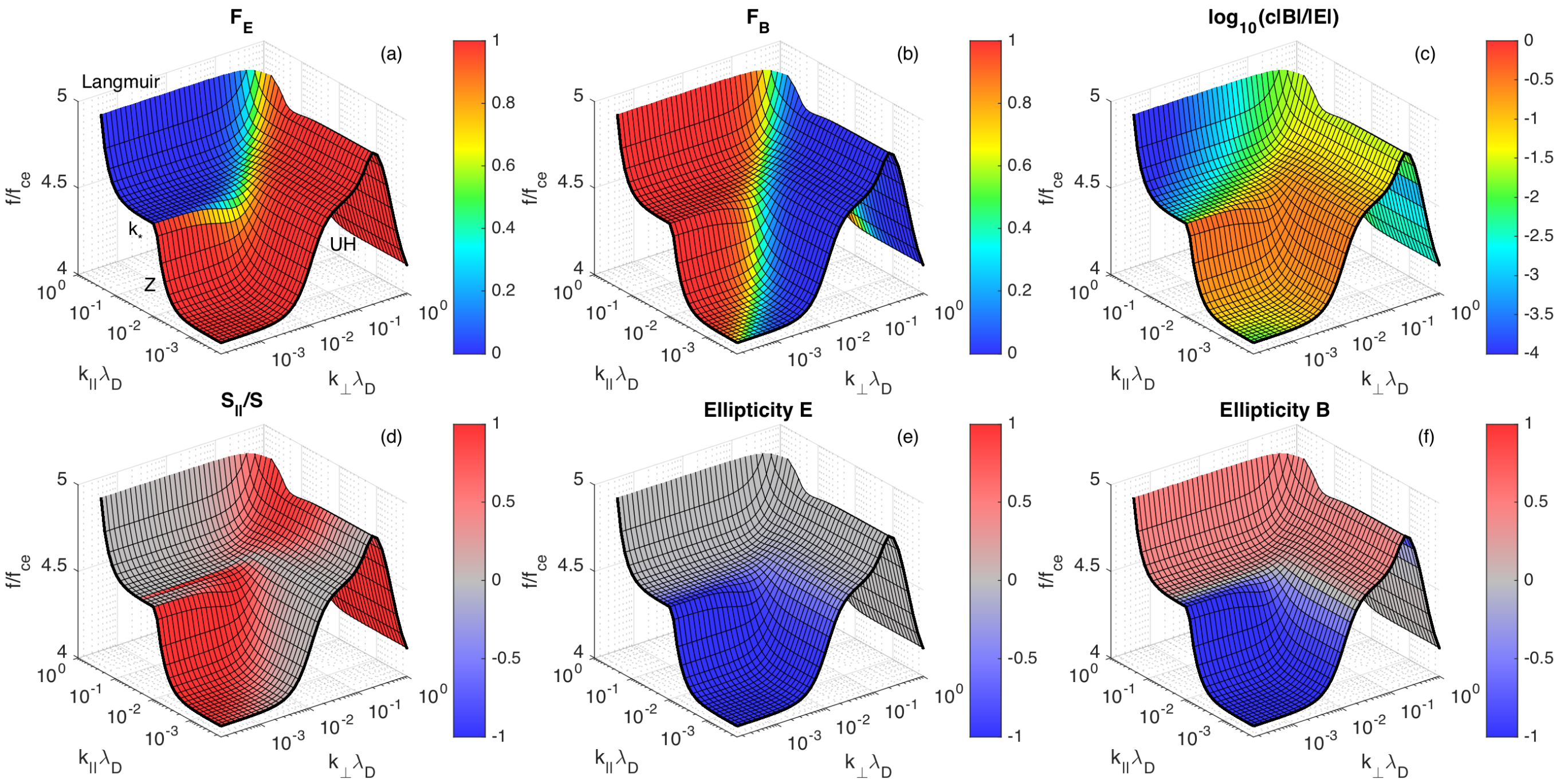
Langmuir/UH dispersion surface

- Single electron Maxwellian distribution.

$$F_E = \frac{\sum E_{\perp}(t)^2}{\sum E_{\perp}(t)^2 + \sum E_{\parallel}(t)^2}$$

$$F_B = \frac{\sum B_{\perp}(t)^2}{\sum B_{\perp}(t)^2 + \sum B_{\parallel}(t)^2}$$

$T_e = 200 \text{ eV}; n_e = 0.5 \text{ cm}^{-3}; B_0 = 50 \text{ nT}$



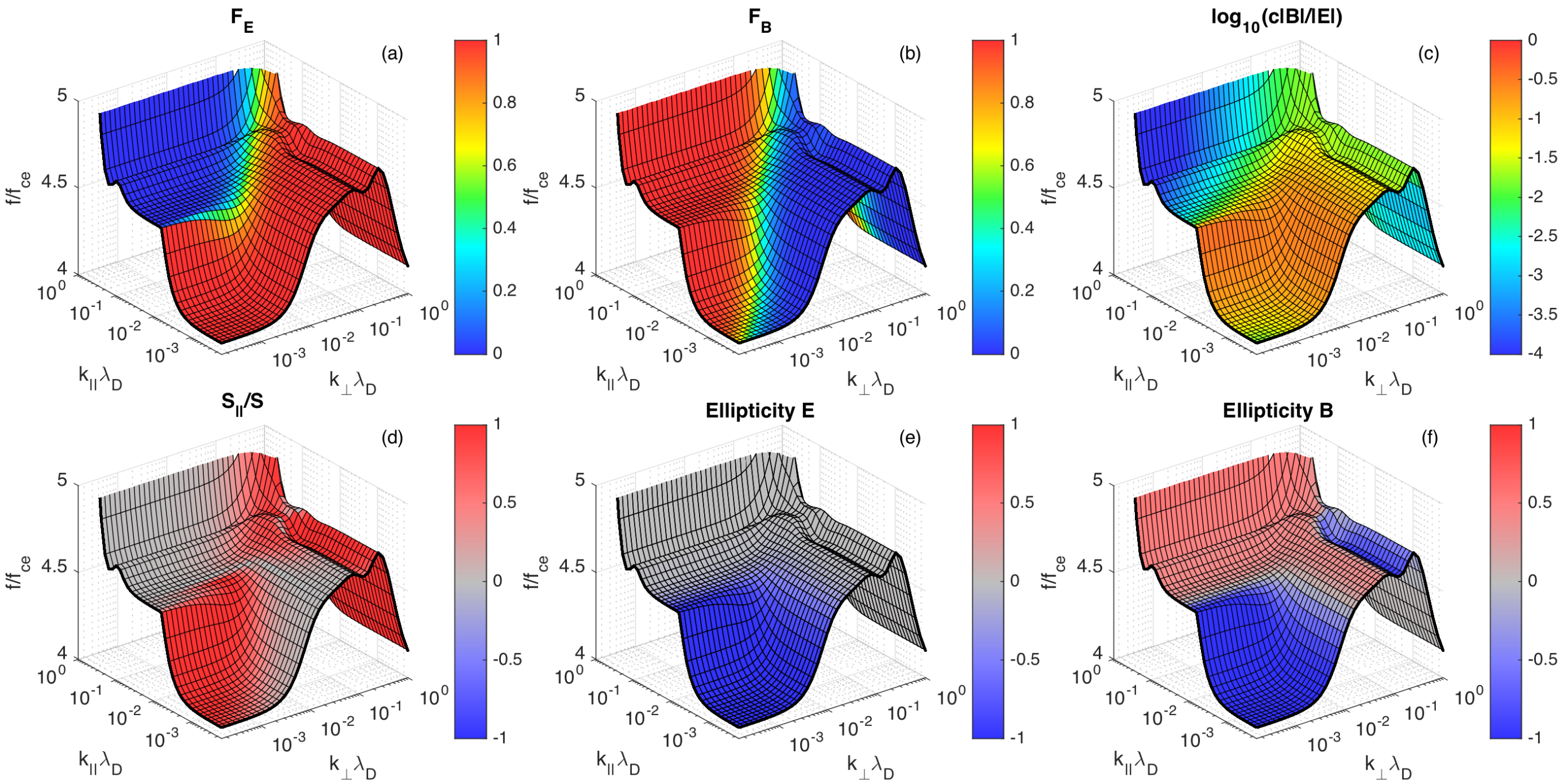
Langmuir/UH dispersion surface

- Hot and cold electron Maxwellian distributions

$n_e = 0.5 \text{ cm}^{-3}$; $n_{ec} = 0.95n_e$; $n_{eh} = 0.05n_e$;
 $T_{ec} = 100 \text{ eV}$; $T_{eh} = 2 \text{ keV}$; $B_0 = 50 \text{ nT}$

$$F_E = \frac{\sum E_{\perp}(t)^2}{\sum E_{\perp}(t)^2 + \sum E_{\parallel}(t)^2}$$

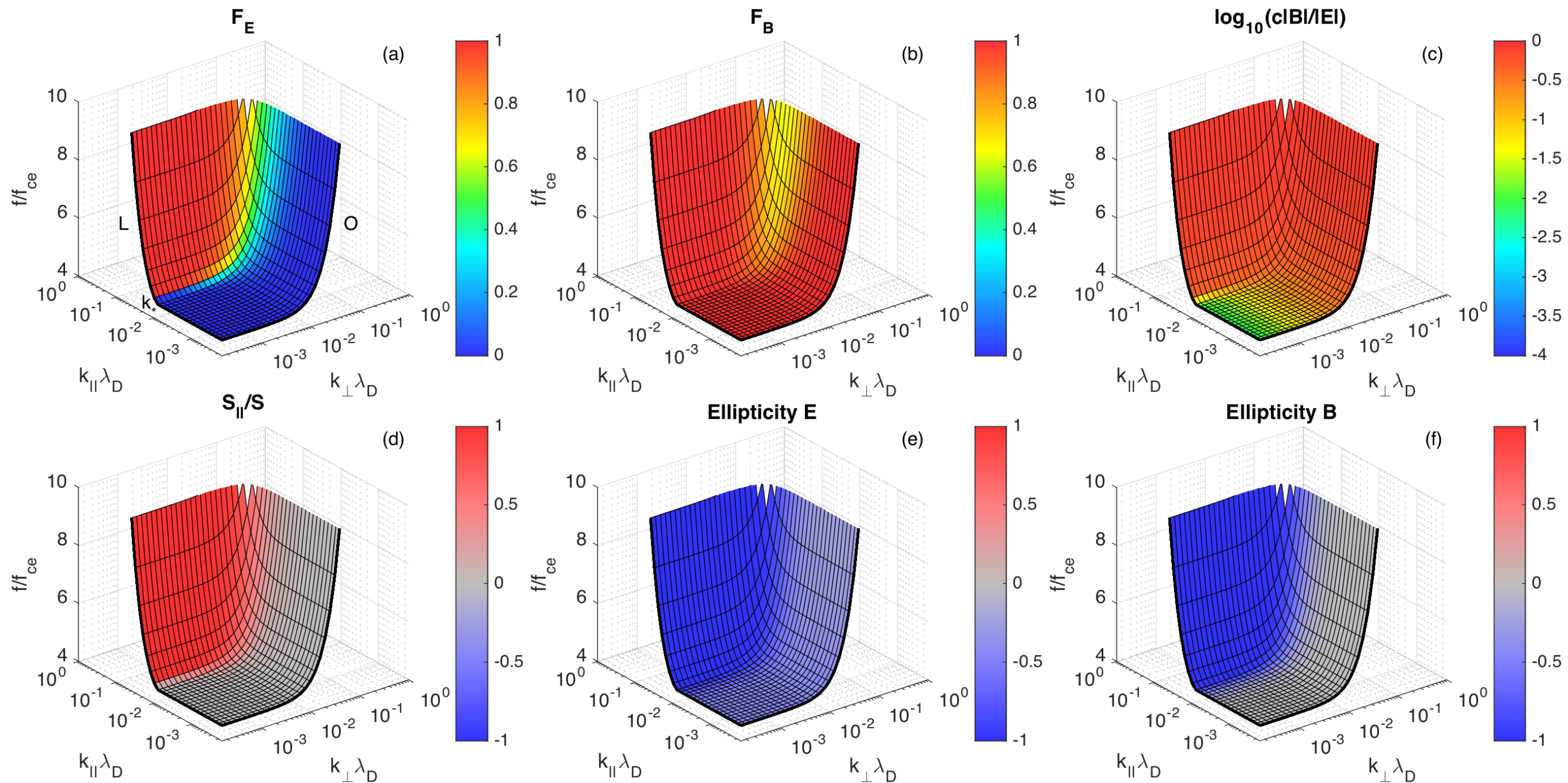
$$F_B = \frac{\sum B_{\perp}(t)^2}{\sum B_{\perp}(t)^2 + \sum B_{\parallel}(t)^2}$$



L-O surface

$$F_E = \frac{\sum E_{\perp}(t)^2}{\sum E_{\perp}(t)^2 + \sum E_{\parallel}(t)^2}$$

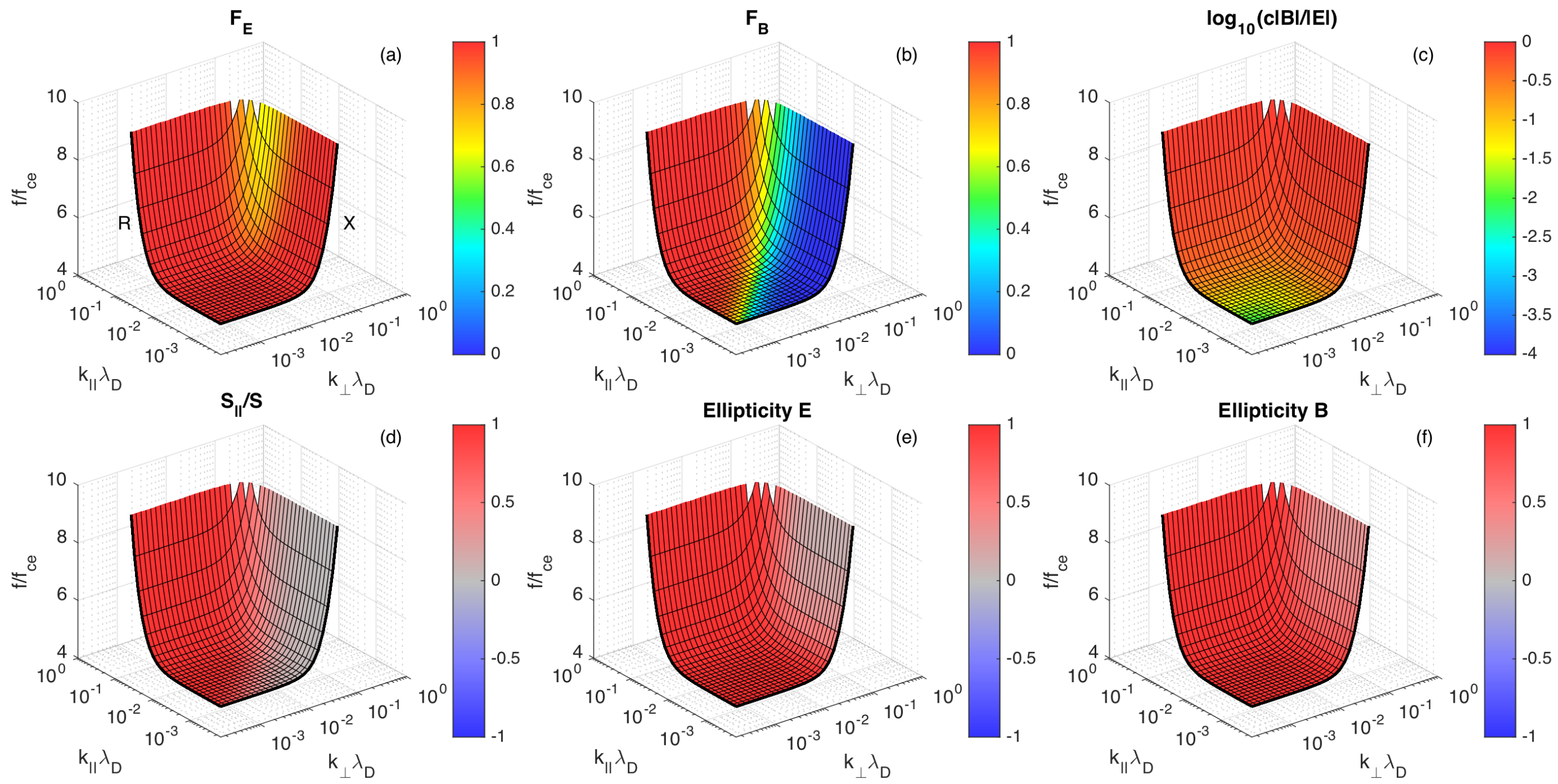
$$F_B = \frac{\sum B_{\perp}(t)^2}{\sum B_{\perp}(t)^2 + \sum B_{\parallel}(t)^2}$$



R-X surface

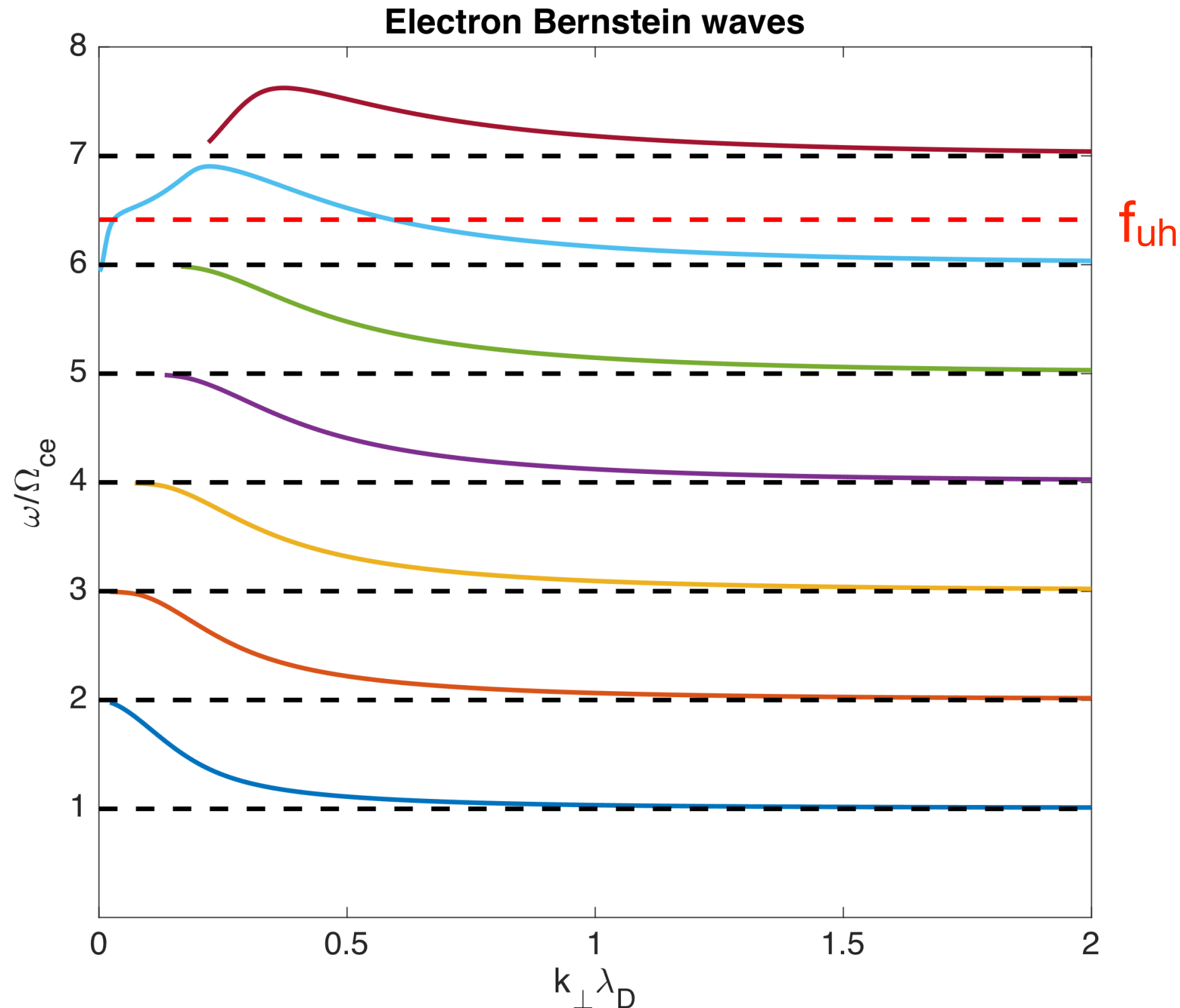
$$F_E = \frac{\sum E_{\perp}(t)^2}{\sum E_{\perp}(t)^2 + \sum E_{\parallel}(t)^2}$$

$$F_B = \frac{\sum B_{\perp}(t)^2}{\sum B_{\perp}(t)^2 + \sum B_{\parallel}(t)^2}$$



Electron Bernstein waves

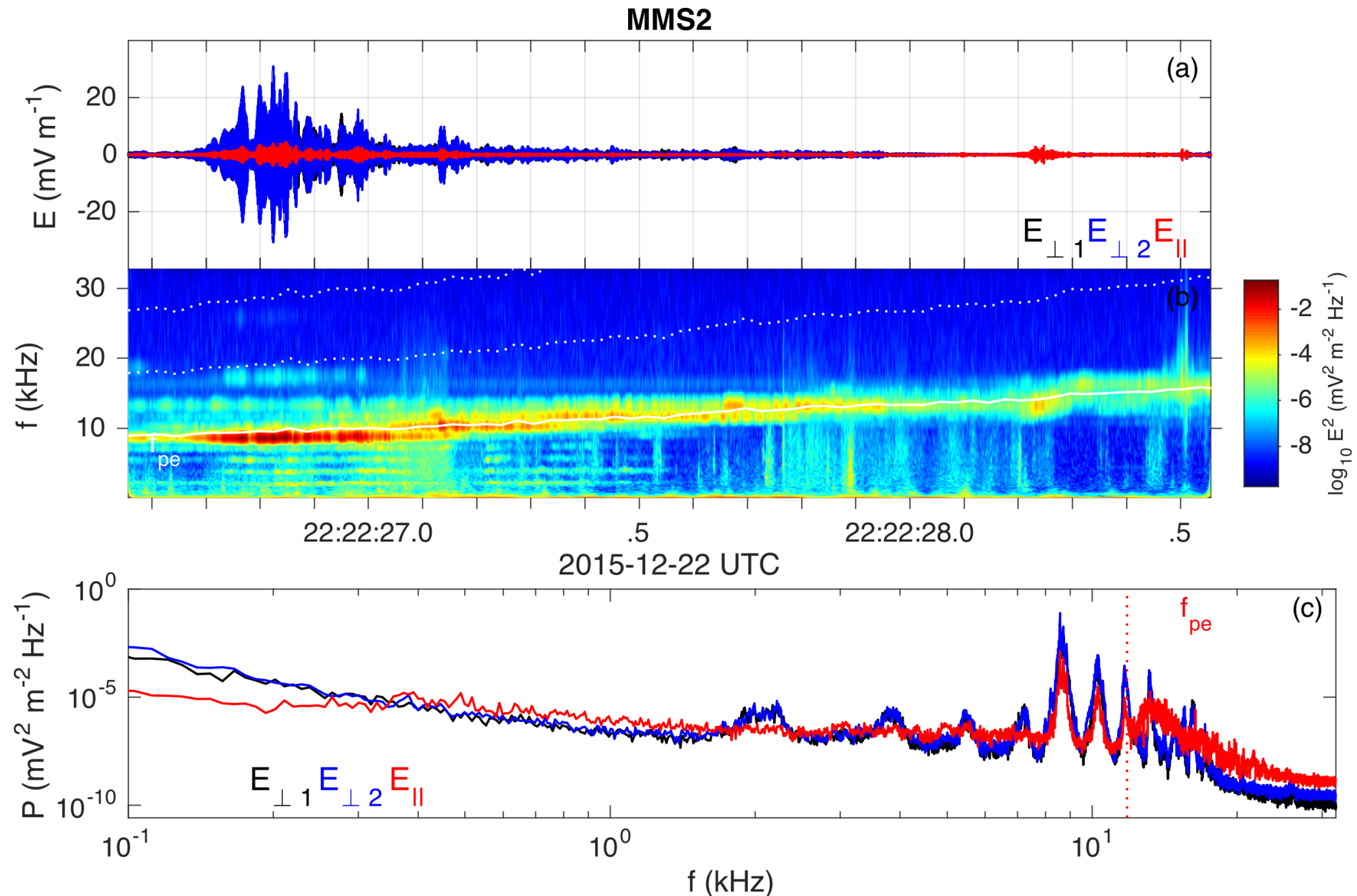
- In addition to the three dispersion surfaces near f_{pe} , electron Bernstein waves can develop between f_{ce} harmonics.



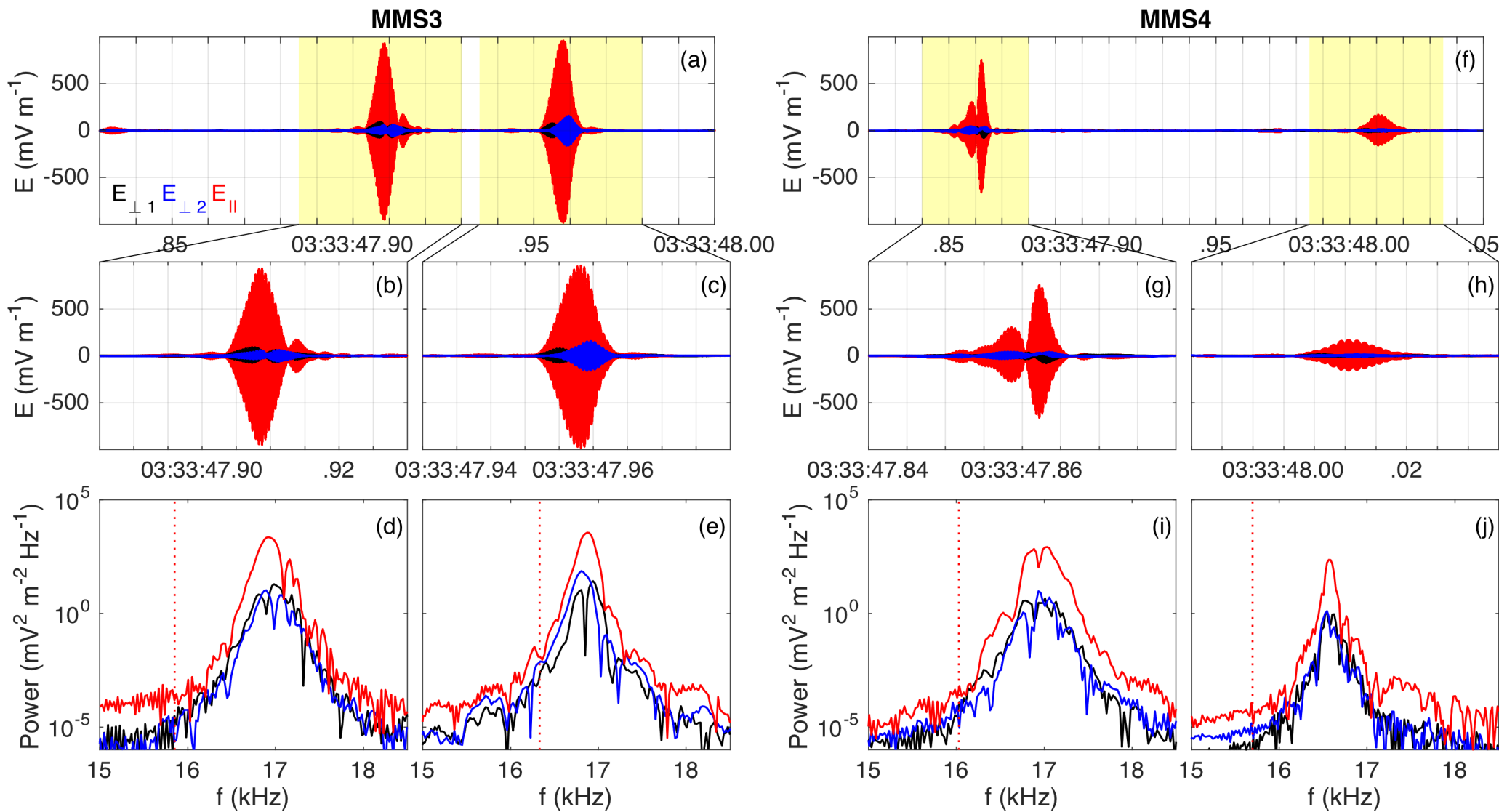
MMS data

- We search through high-resolution electric field data for large-amplitude waves near f_{pe} ($E_{\max} > 20 \text{ mV m}^{-1}$).
- From MMS magnetopause phases we find 8837 wave events (most near the MP, some near the foreshock).

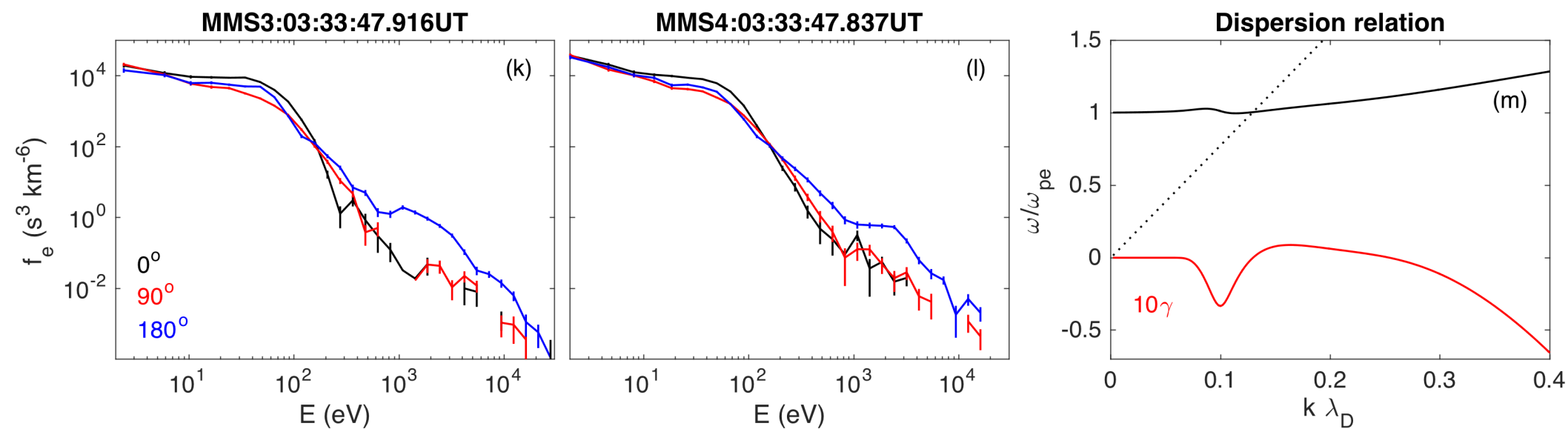
Example wave event near the magnetopause



Langmuir waves (1)



- $E_{\parallel} \gg E_{\perp}$



- Langmuir waves are driven by the bump-on-tail instability.

Langmuir waves (2)

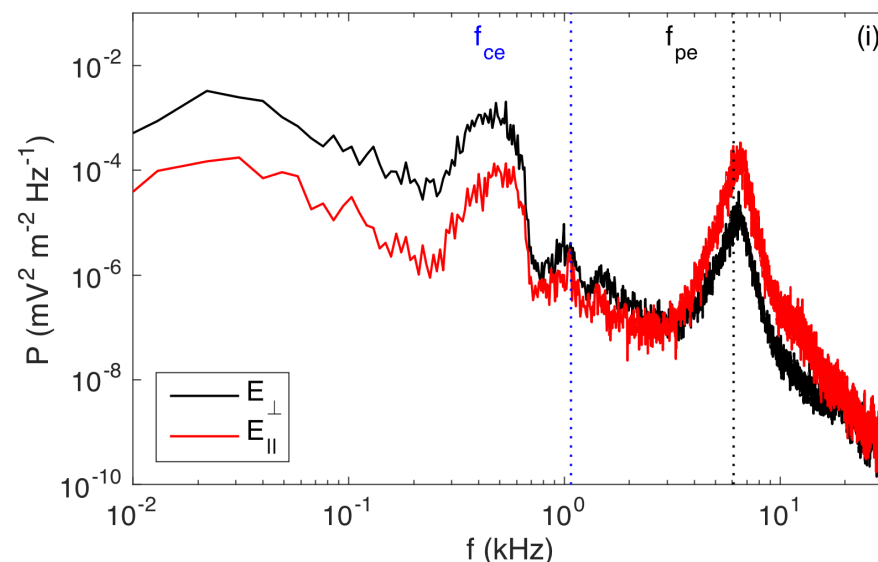
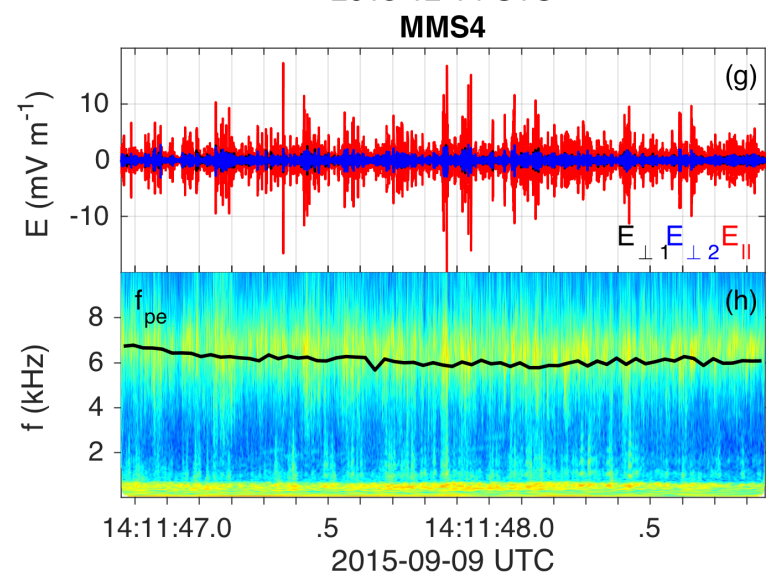
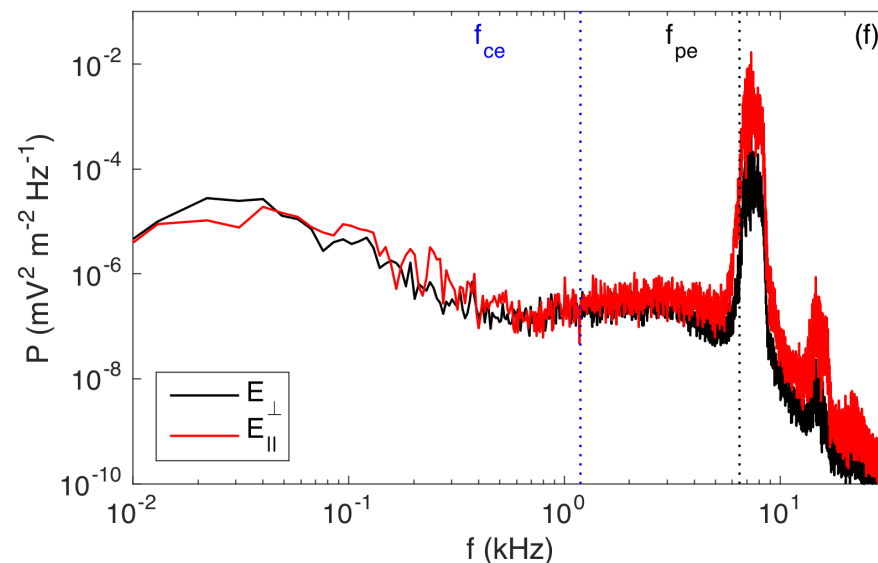
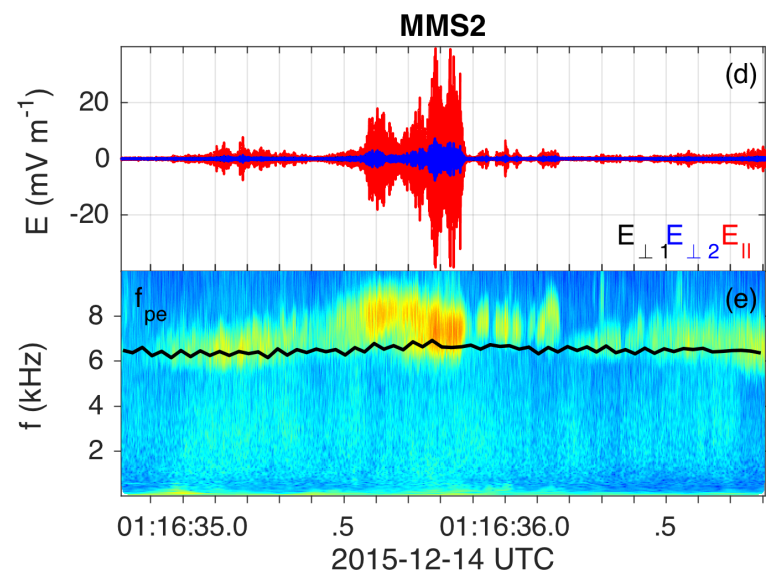
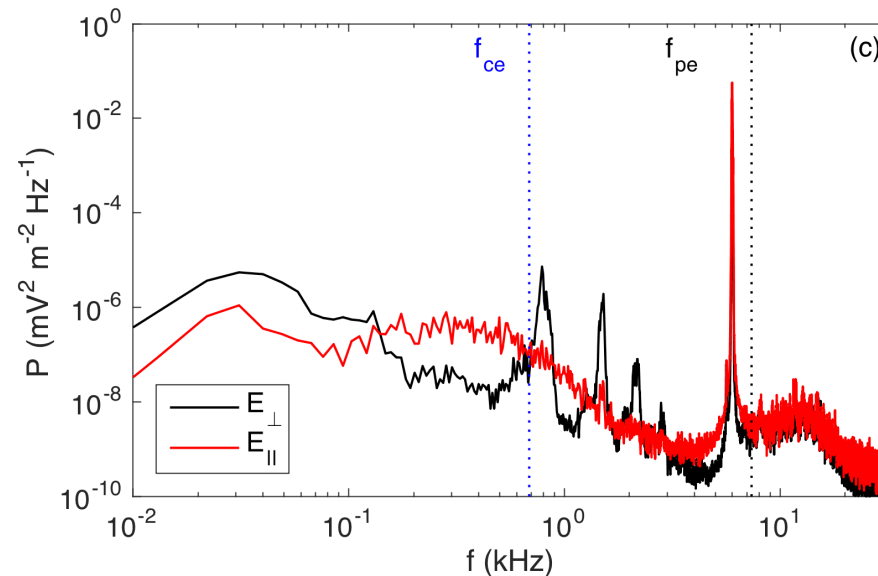
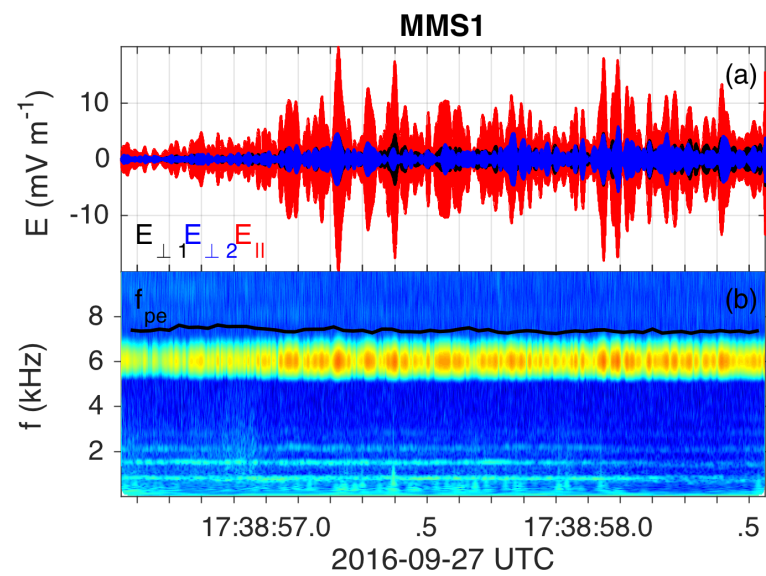
- Three examples of Langmuir waves

Very narrow spectral peak and Bernstein waves.

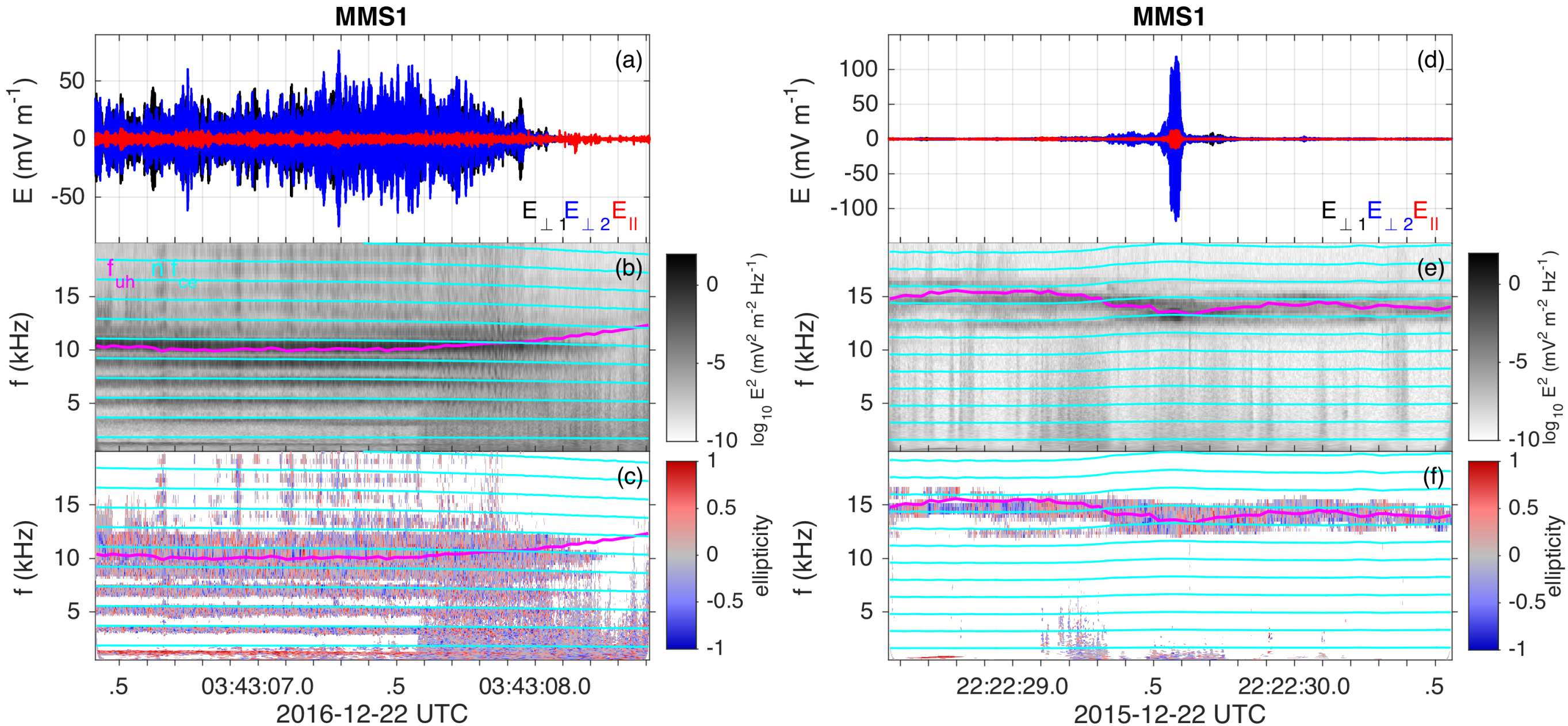
Broader spectral peak Langmuir waves.

Broad spectral peak Langmuir waves and whistler waves.

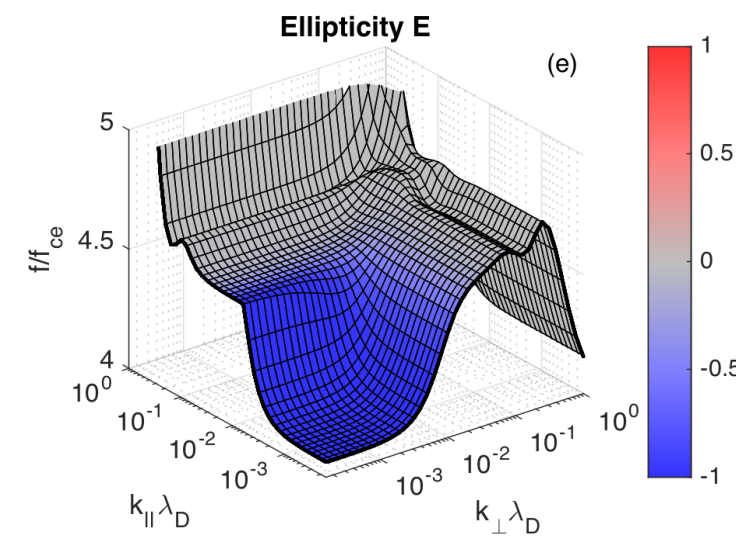
[cf., Reinleitner et al.1982]



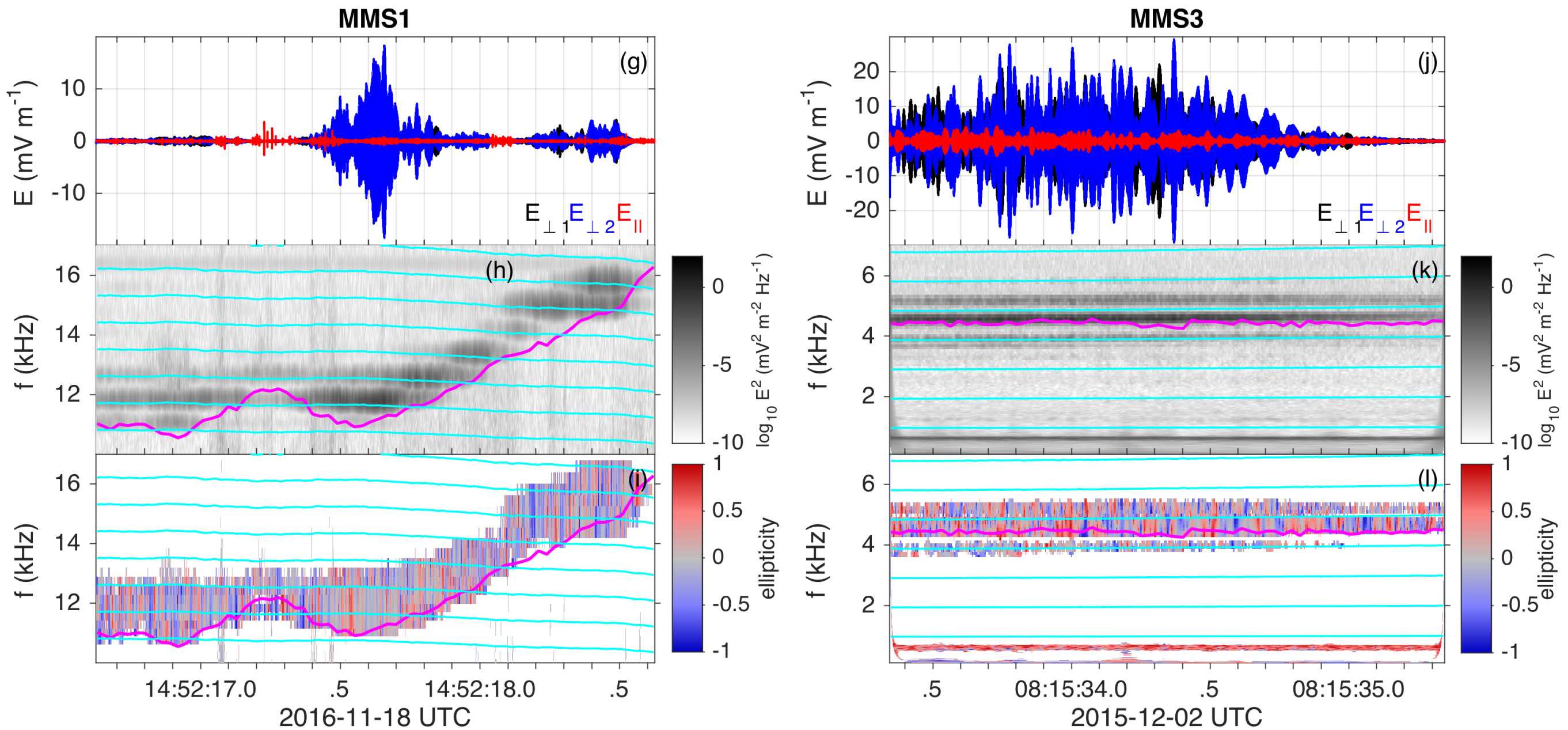
UH waves (1)



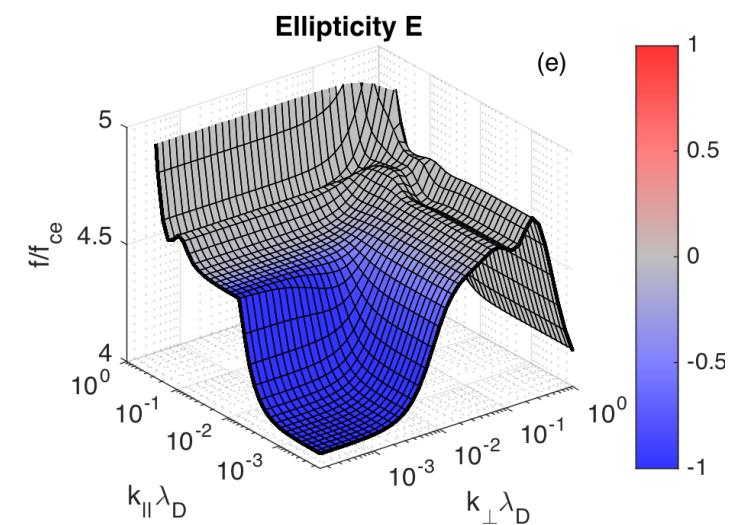
- $E_{\parallel} \ll E_{\perp}$.
- UH waves are can be simultaneously observed with Bernstein waves and whistlers.



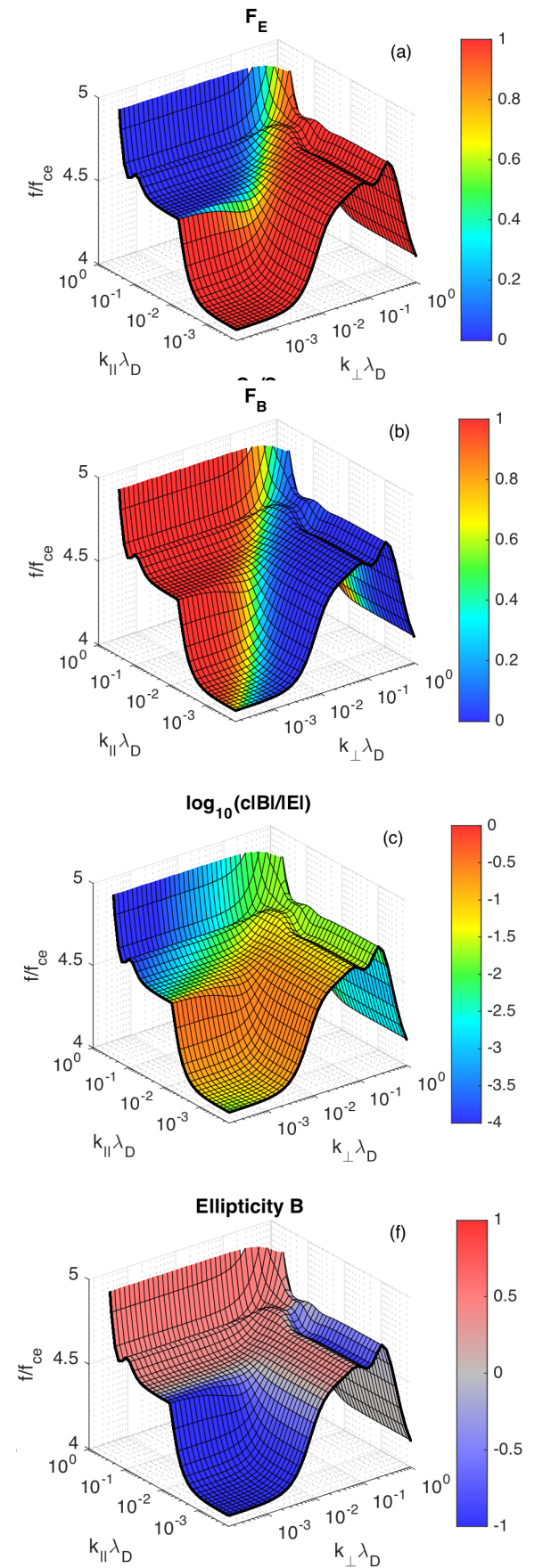
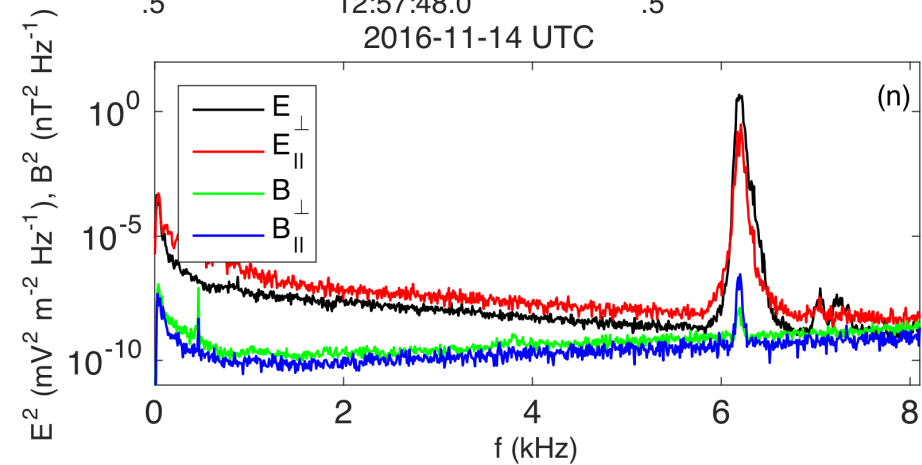
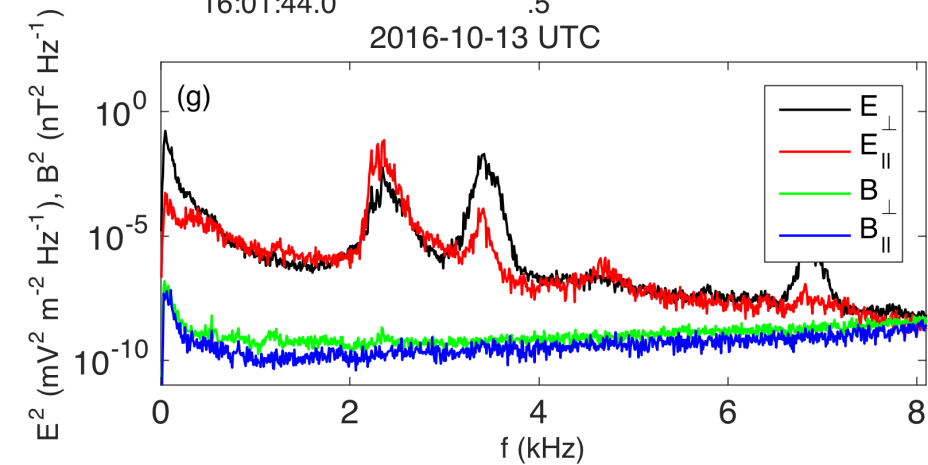
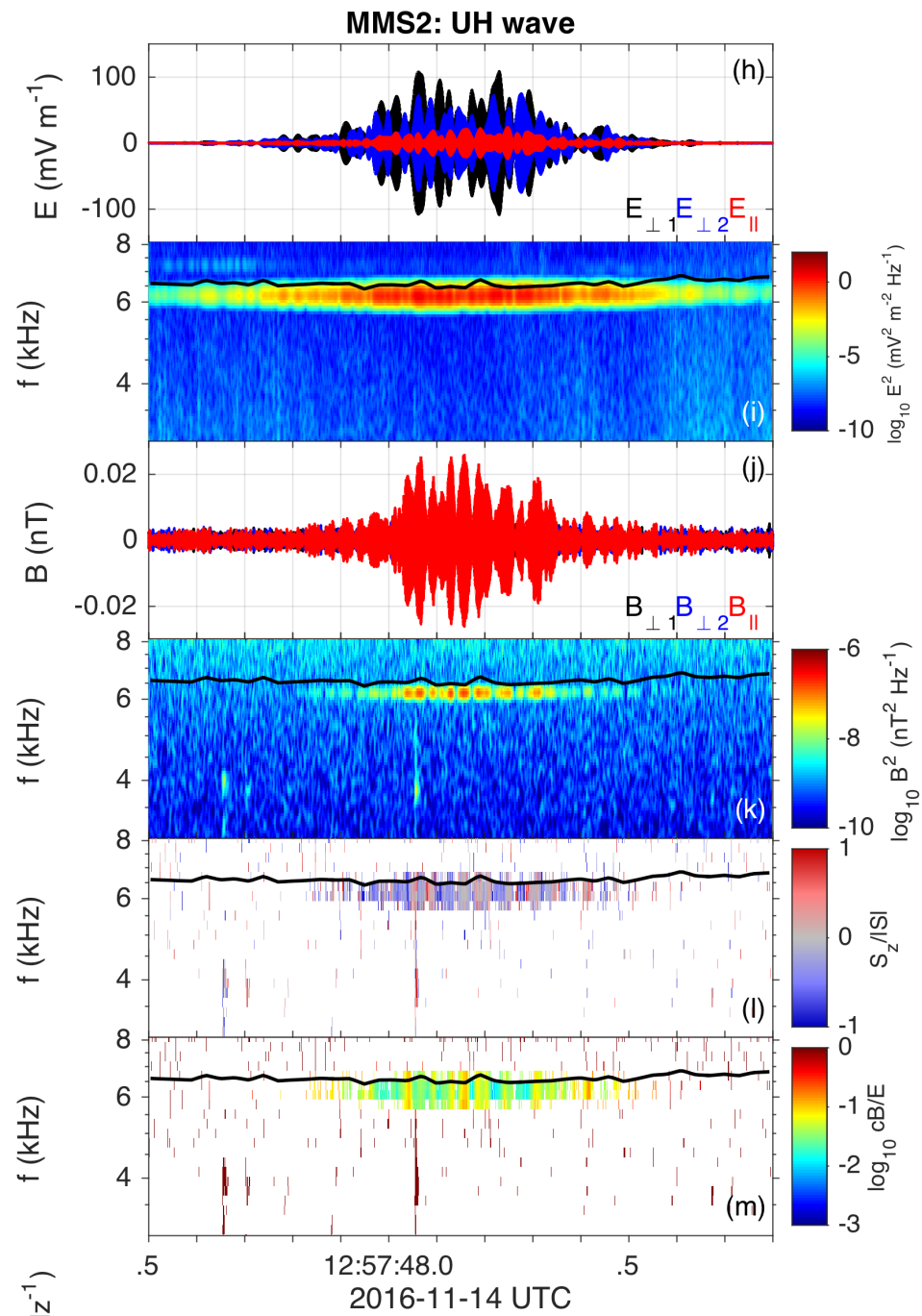
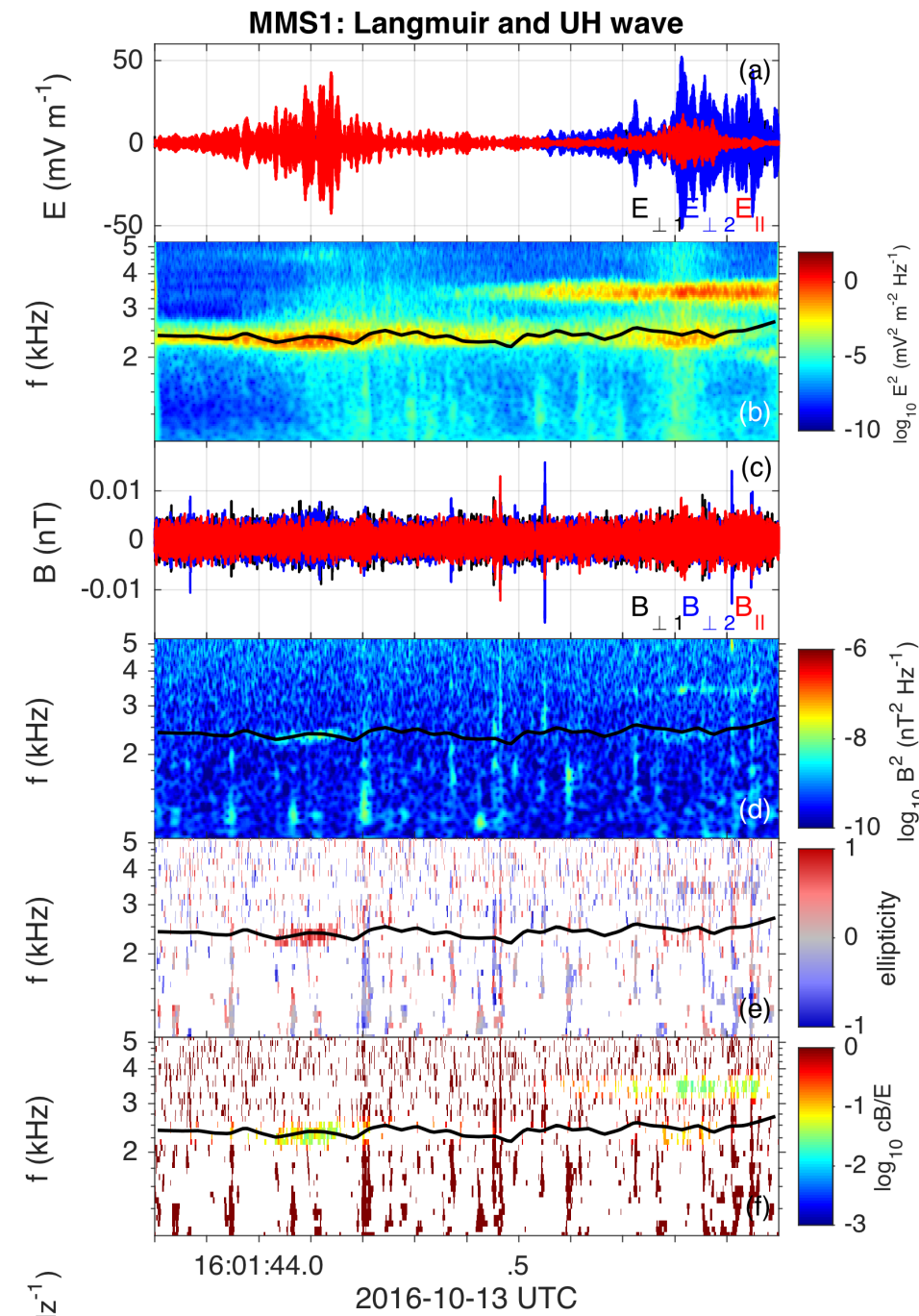
UH waves (2)



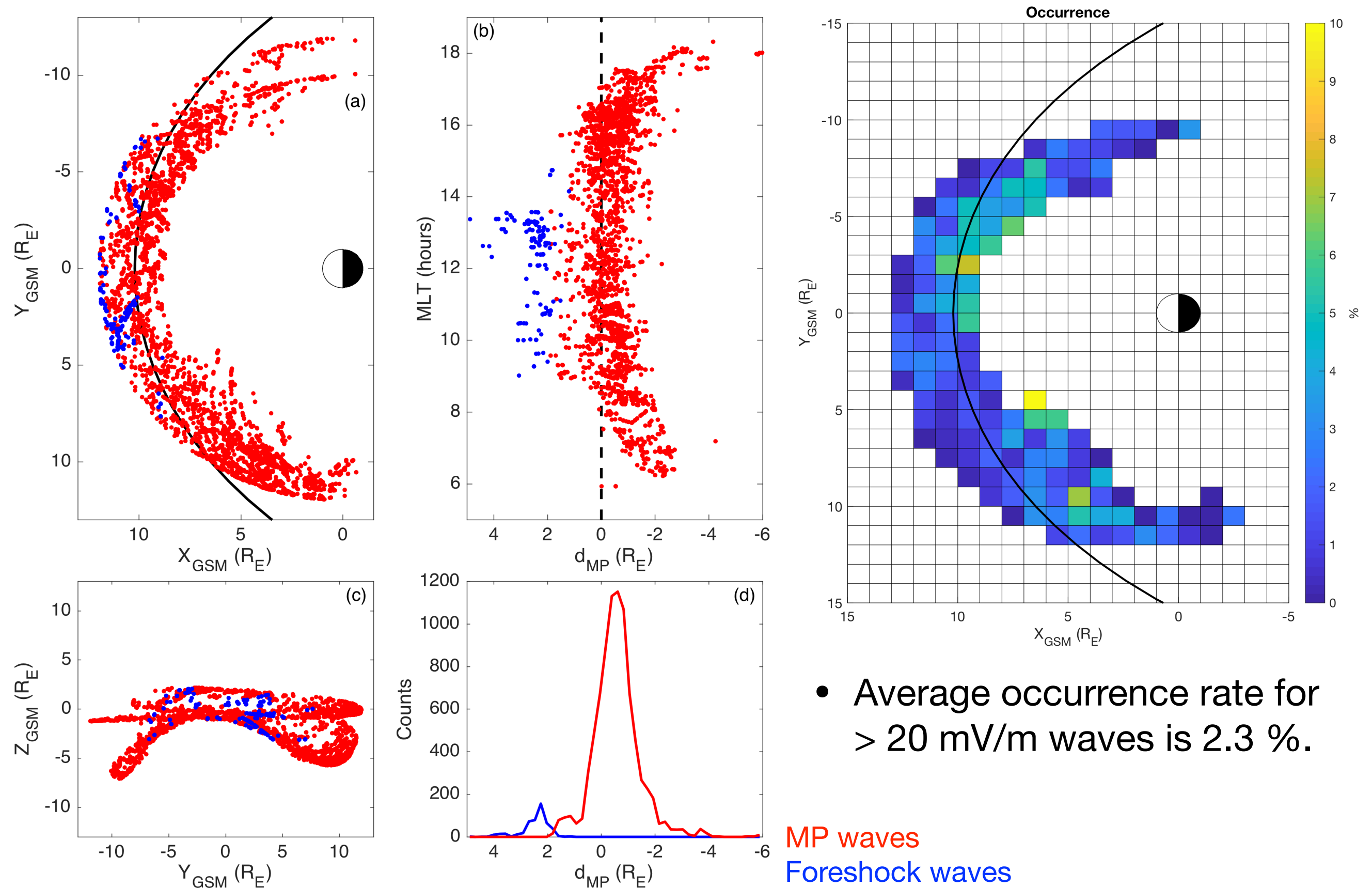
- $E_{\parallel} \ll E_{\perp}$.
- UH waves are can be simultaneously observed with Bernstein waves and whistlers.



Electromagnetic properties



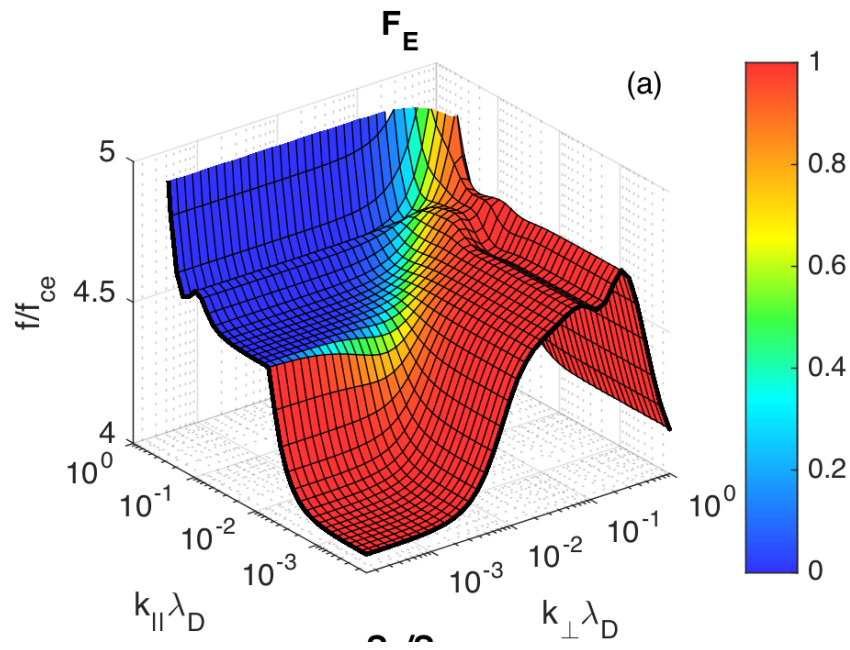
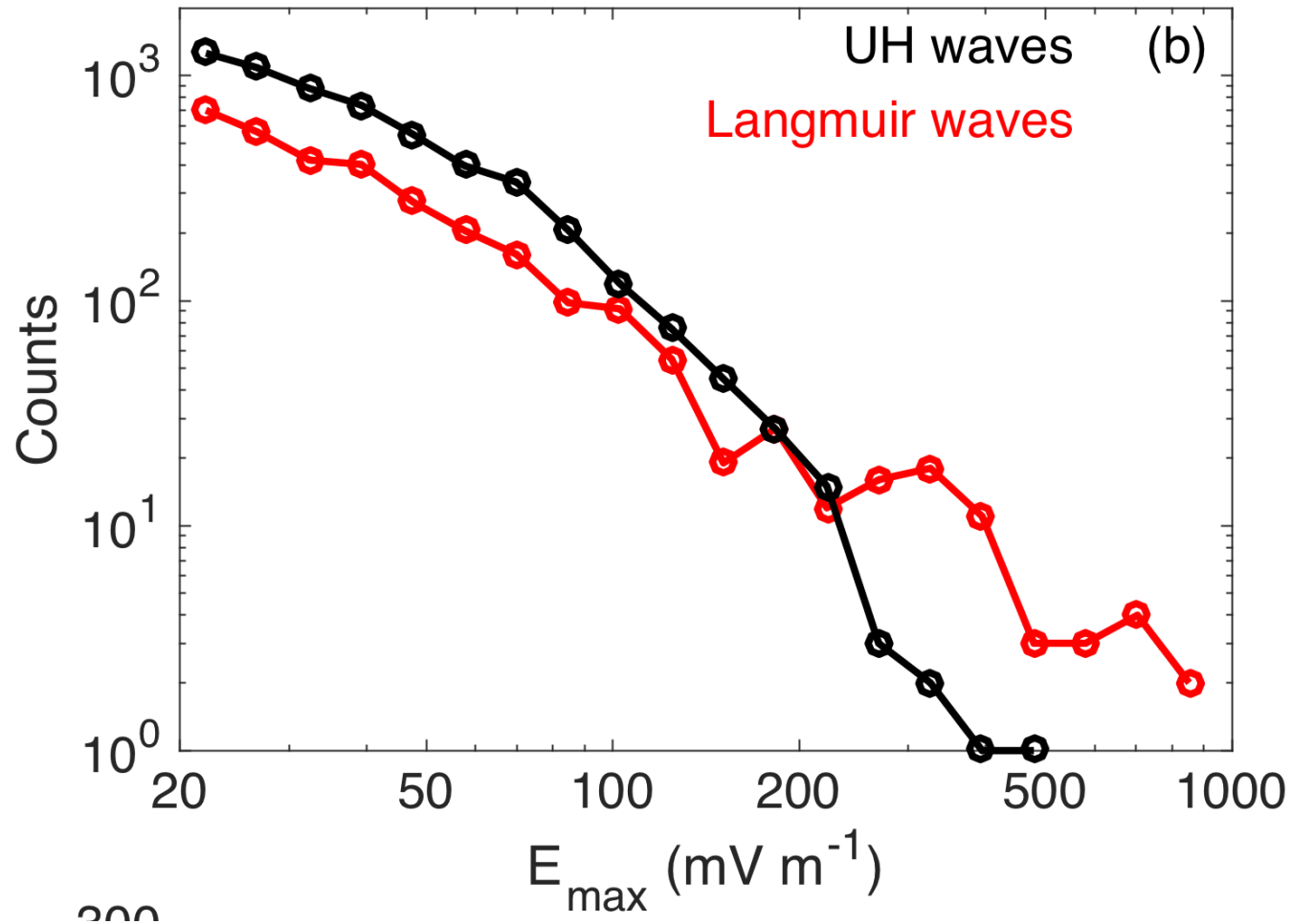
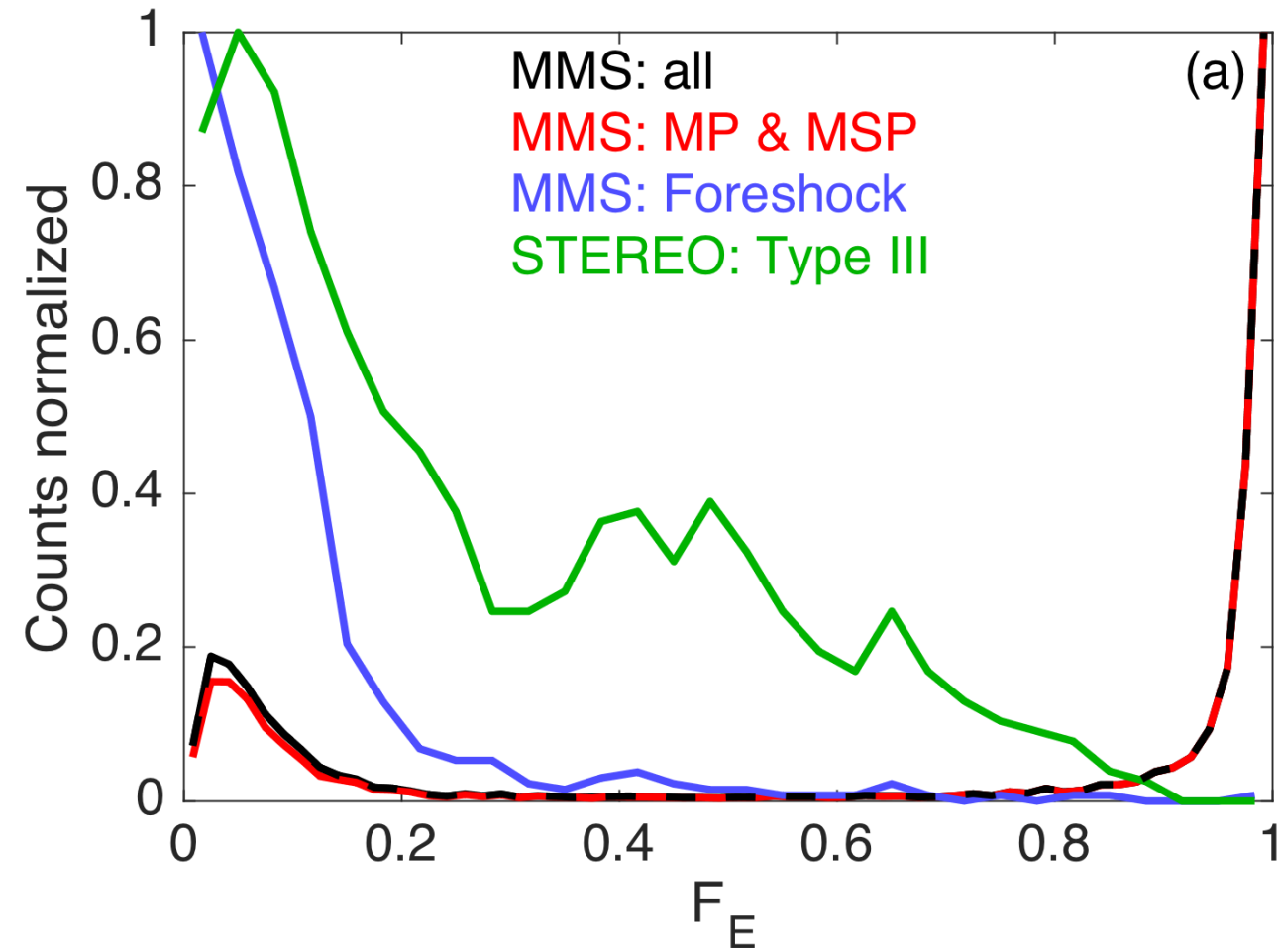
Wave locations



Wave properties (1)

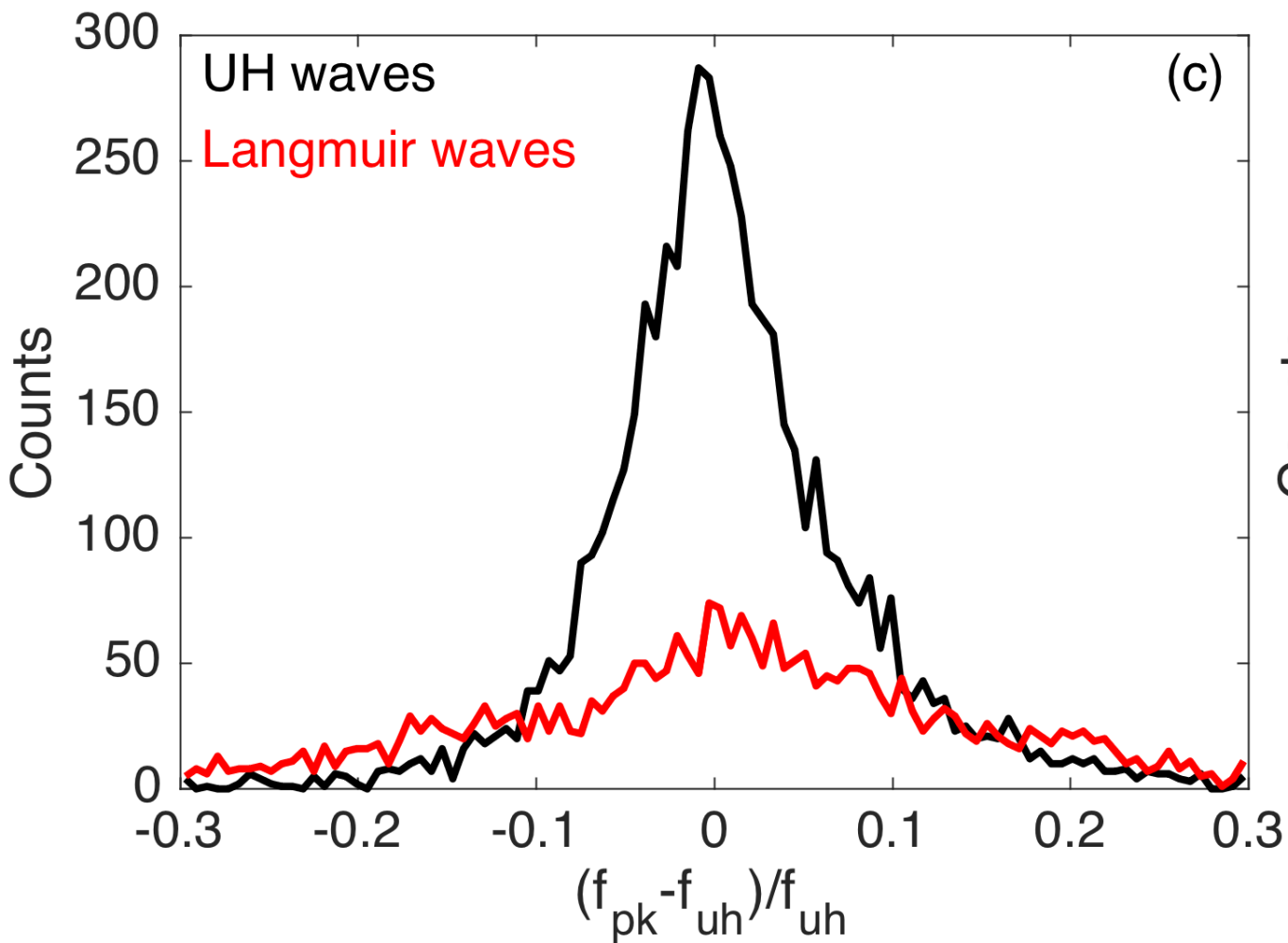
Langmuir waves

$$F_E = \frac{\sum E_{\perp}(t)^2}{\sum E_{\perp}(t)^2 + \sum E_{\parallel}(t)^2} \quad \text{UH waves}$$



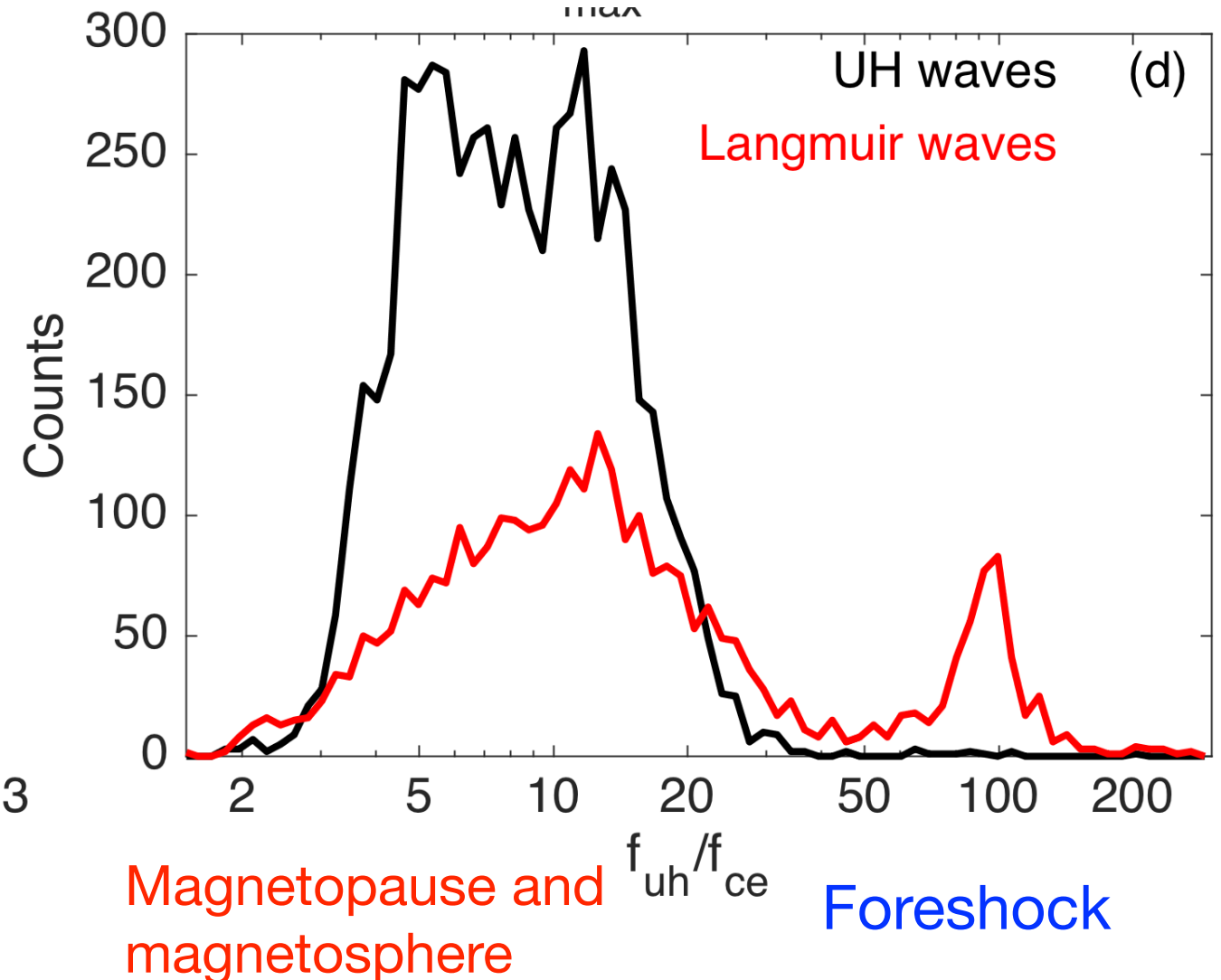
F_E histogram changes depending on region.

Wave properties (2)



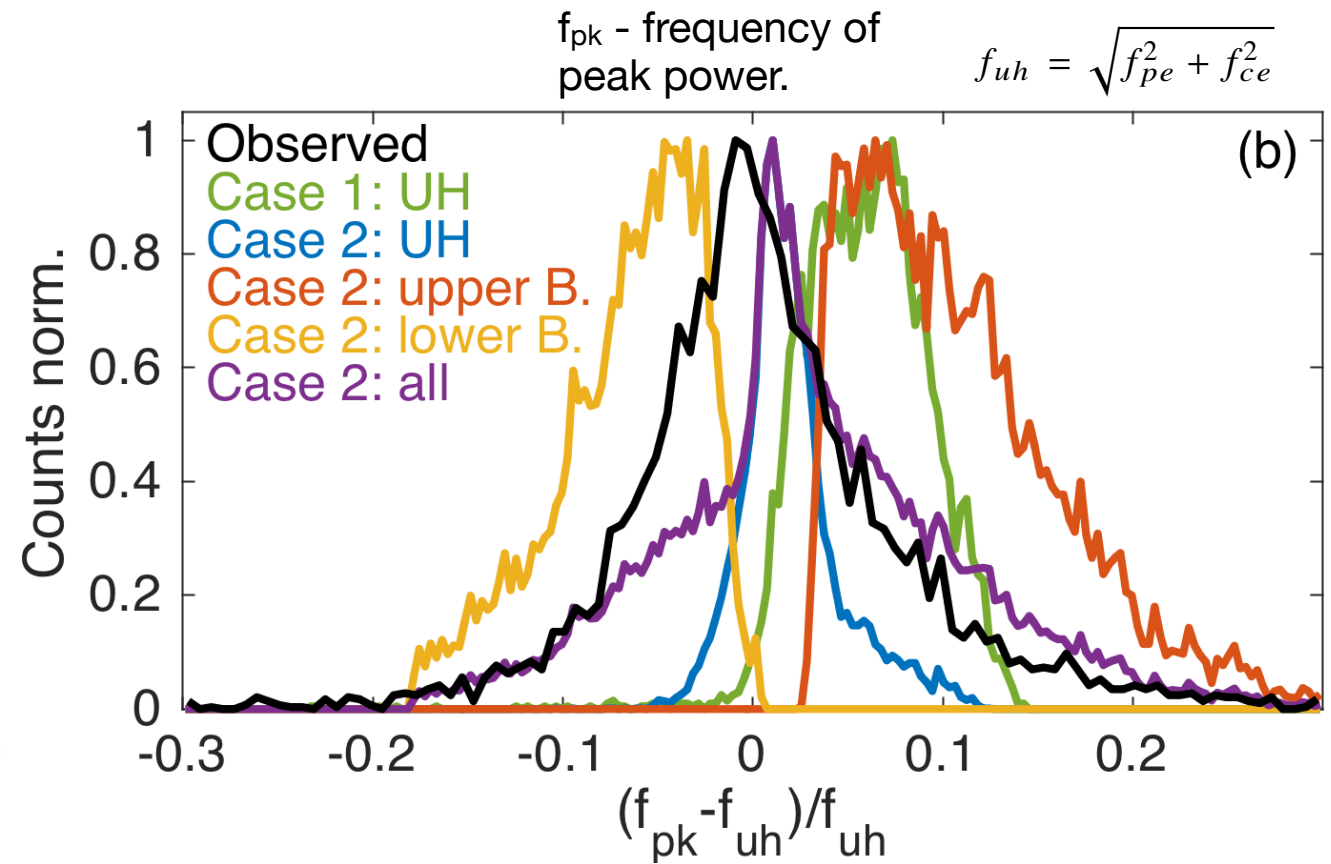
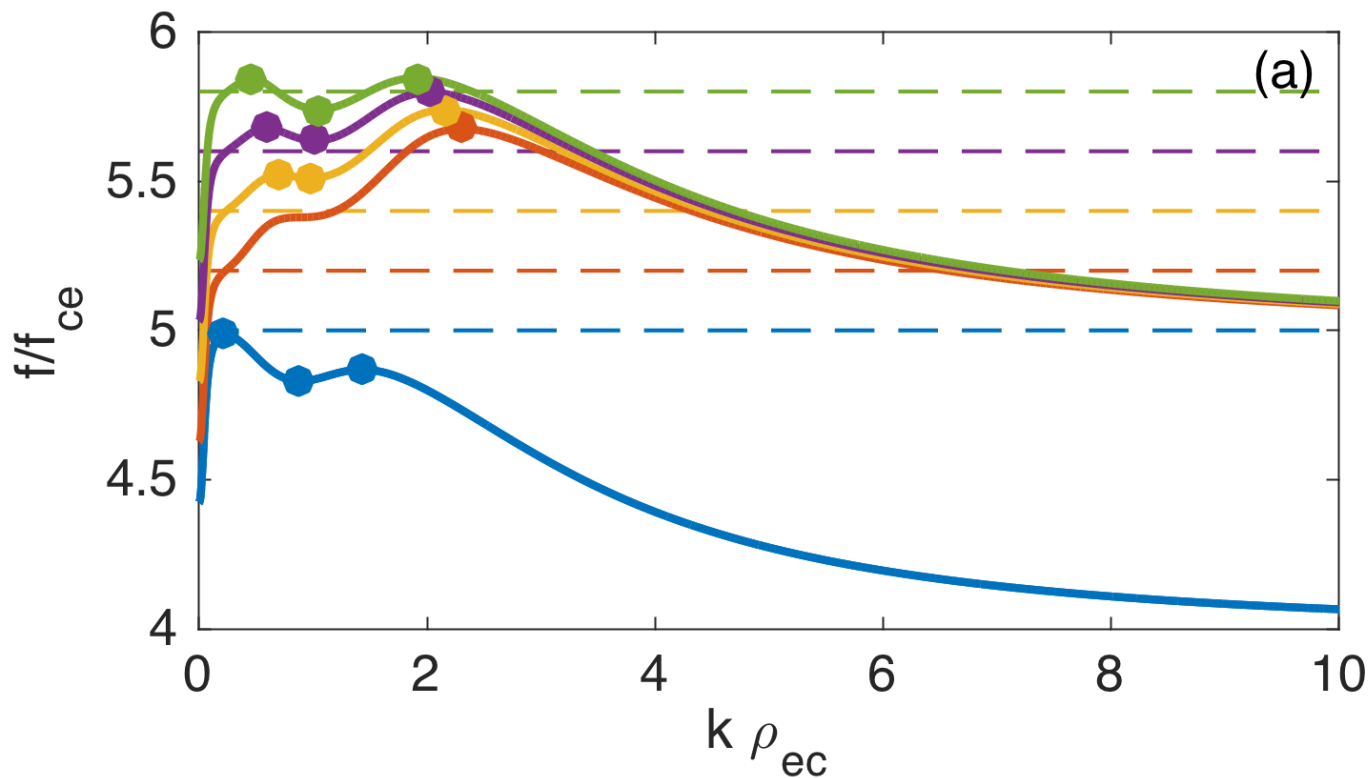
$$f_{uh} = \sqrt{f_{pe}^2 + f_{ce}^2}$$

f_{pk} - frequency
of peak power.



- UH waves are more likely to be found than Langmuir waves at the magnetopause.

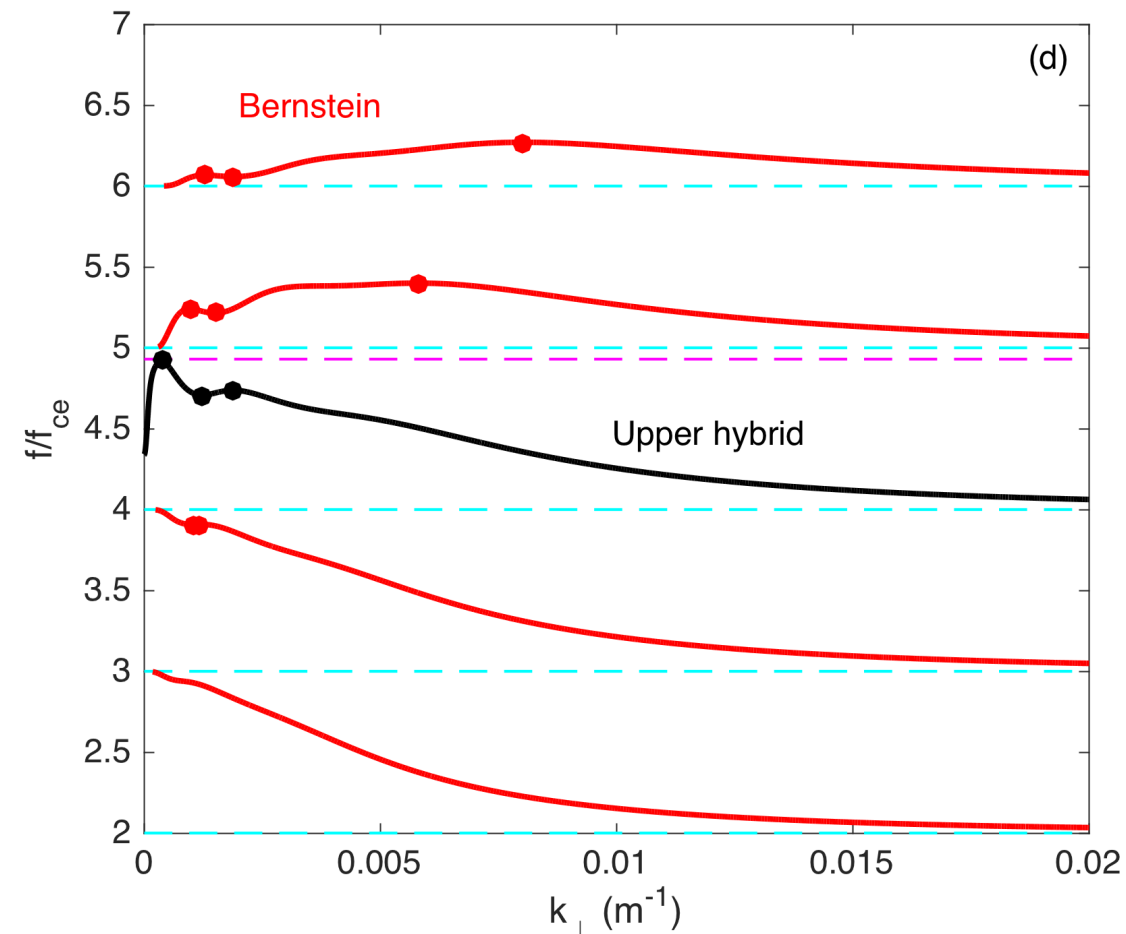
Comparison with kinetic theory



- Case 1: Single Maxwellian - using measured parameters
- Case 2: Hot and Cold Maxwellians - measured B and n.

We assume f_{pk} occurs where $v_g = 0$.

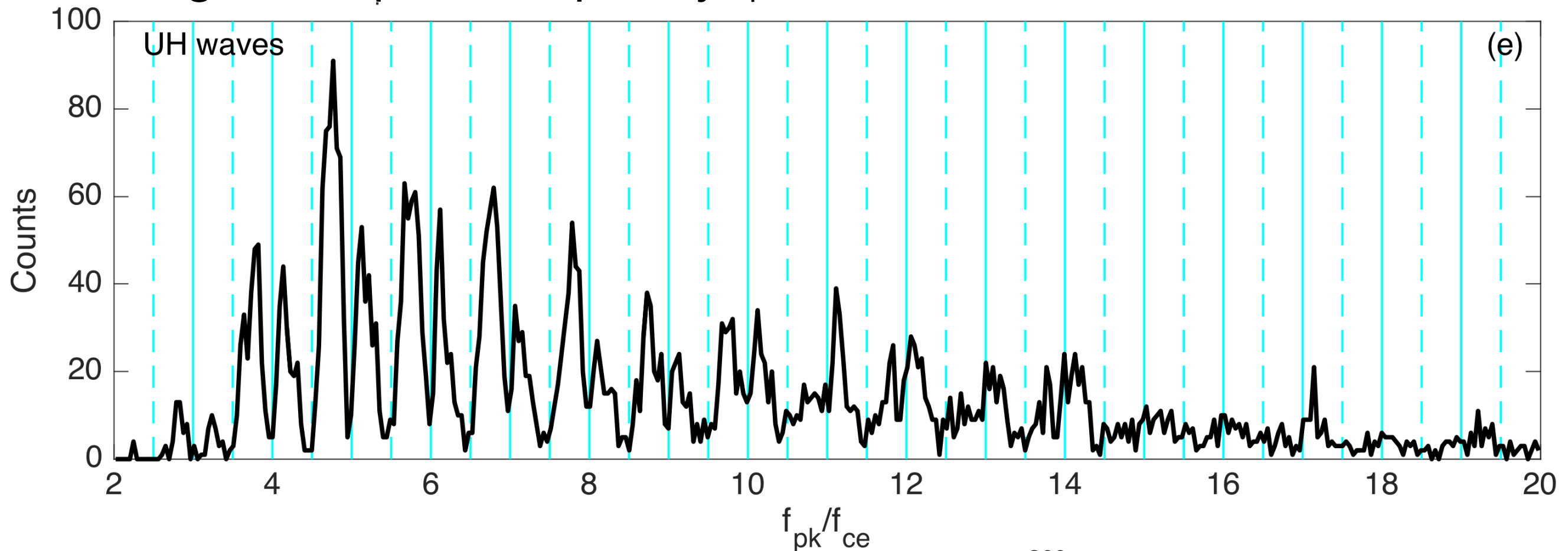
- Case 1 waves do not agree well with observations.
- Case 2 agrees well with observations.



Wave properties (3)

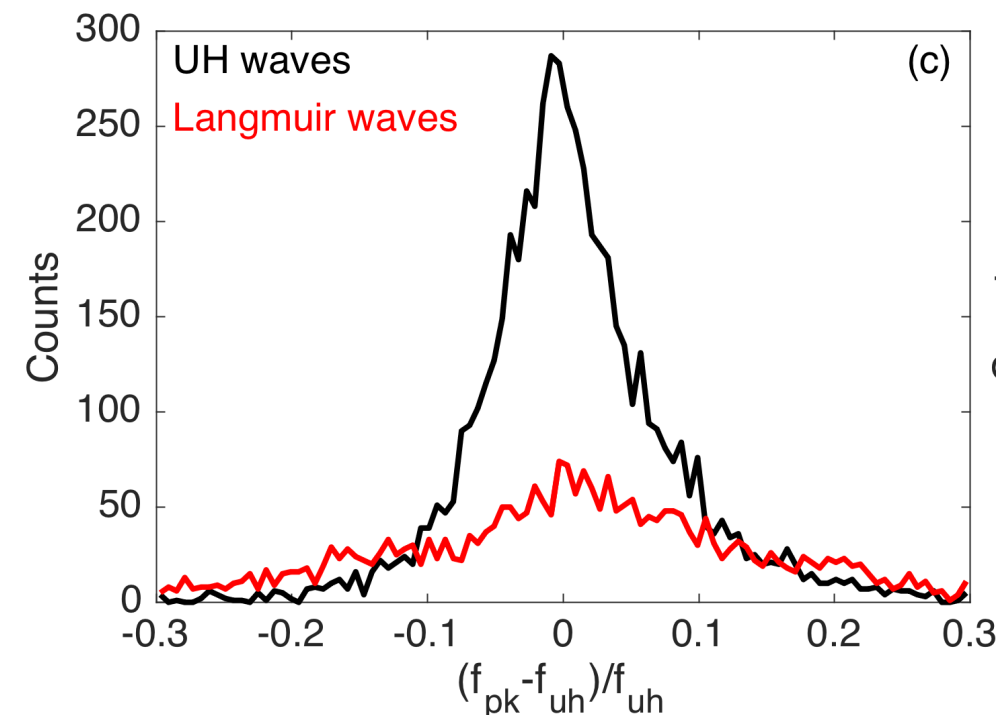
Histogram of peak frequency f_{pk}/f_{ce} for UH waves

f_{pk} - frequency of peak power.



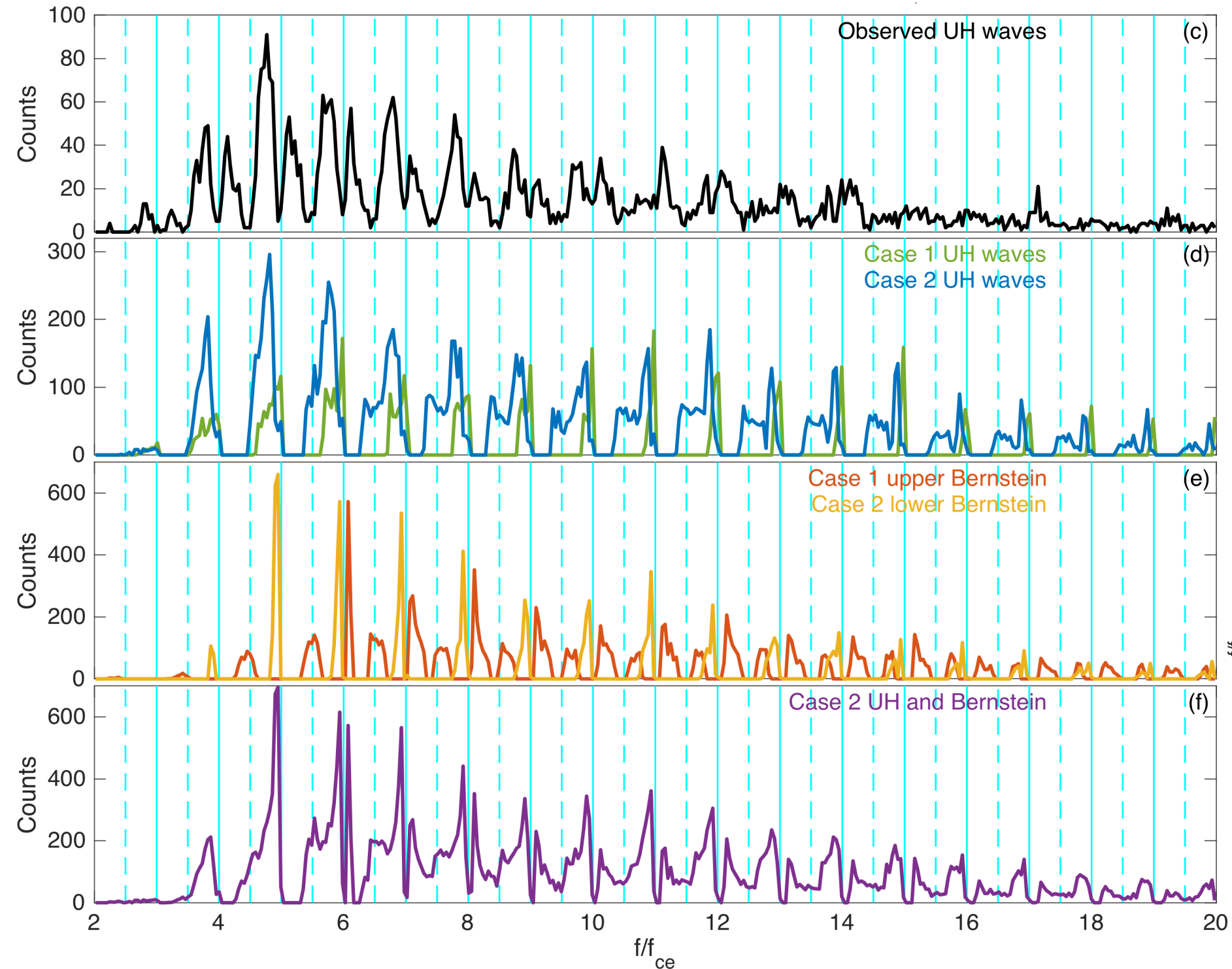
- Peak frequencies of UH waves tend to avoid nf_{ce} and $(n+1/2)f_{ce}$.

This behavior can explain some of the spread in $(f_{pk} - f_{uh})/f_{uh}$.

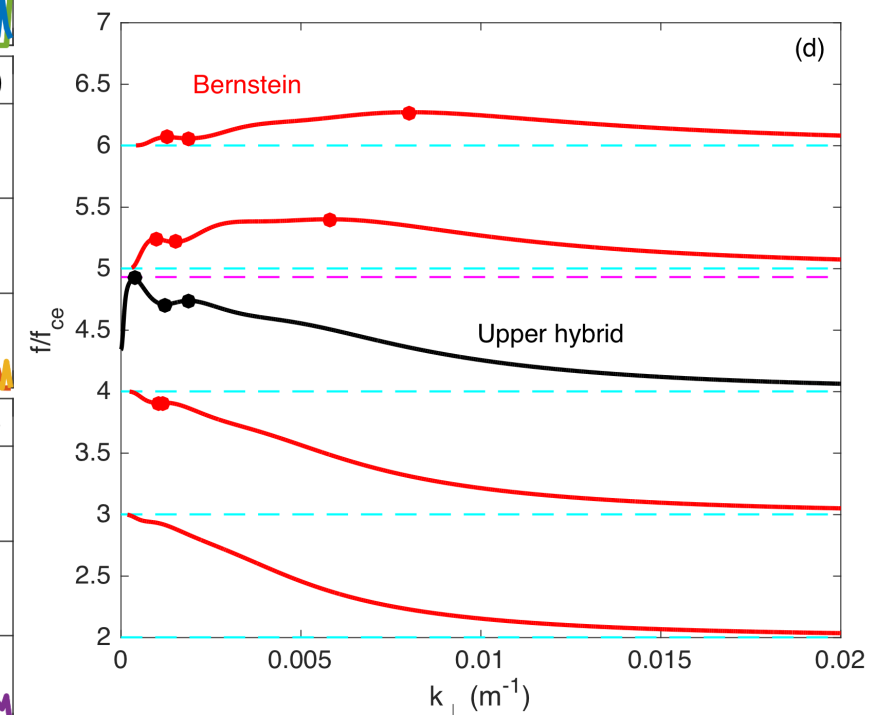


Comparison with kinetic theory

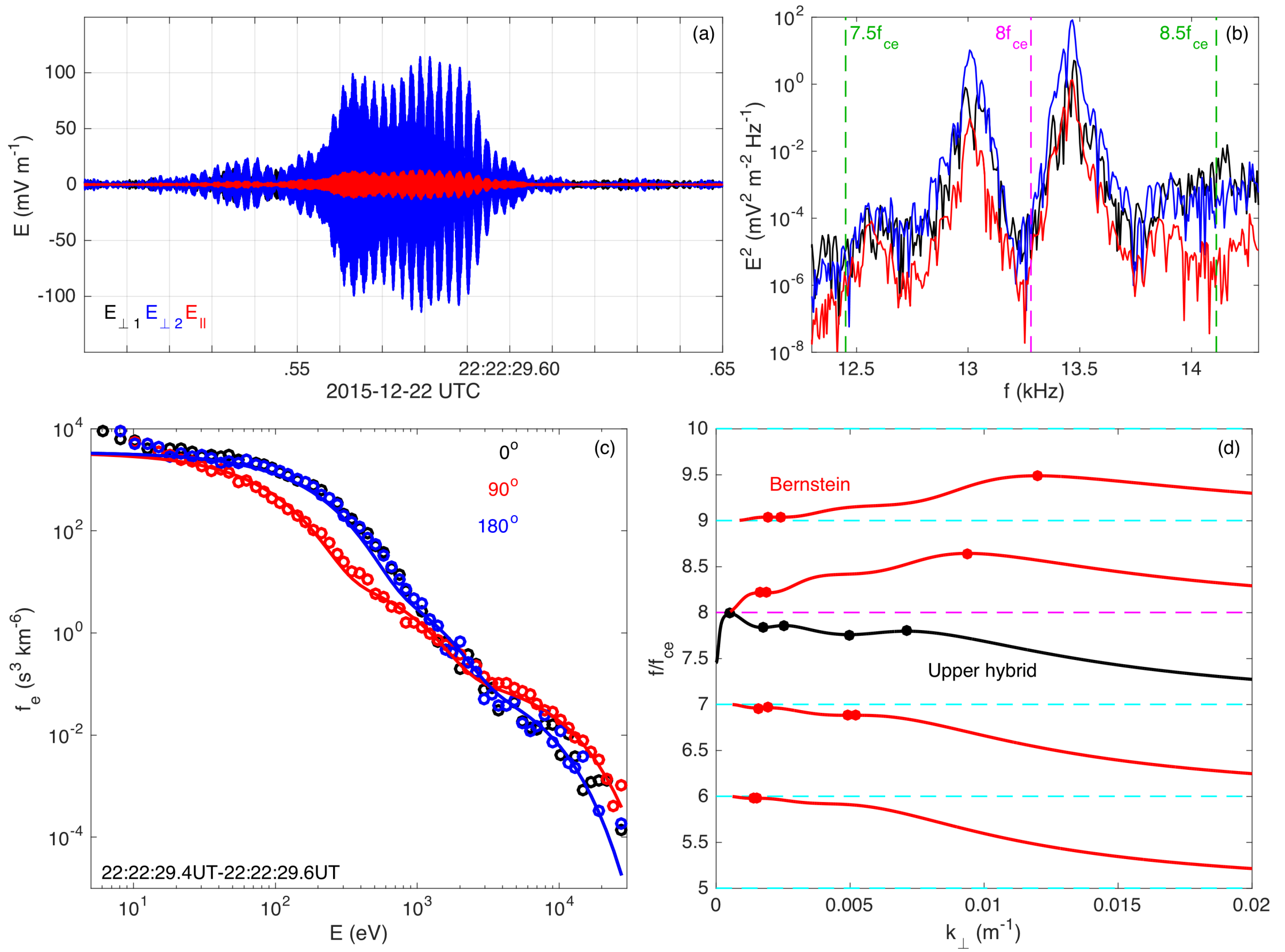
- Case 1: Single Maxwellian
- Case 2: Hot and Cold Maxwellians



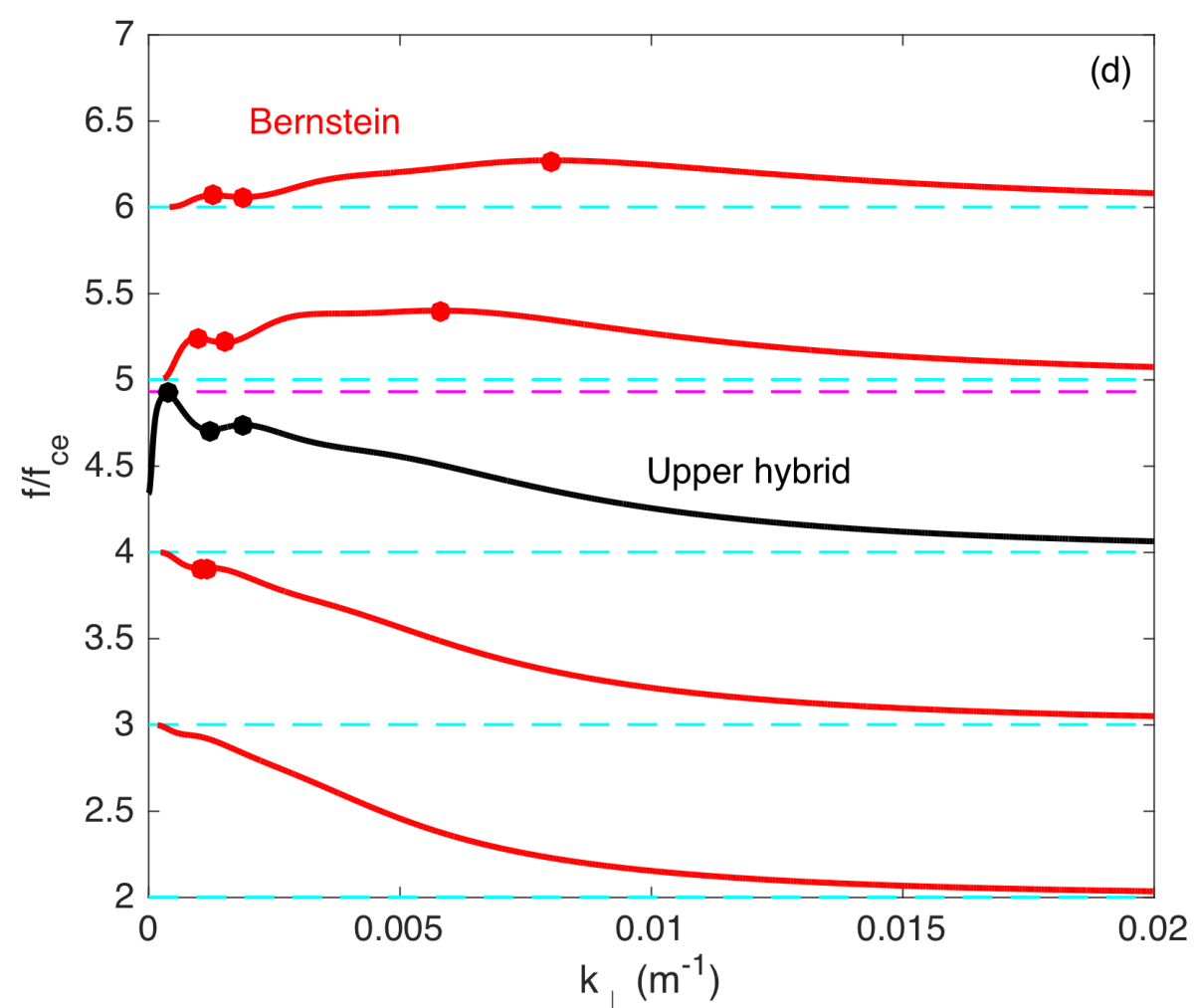
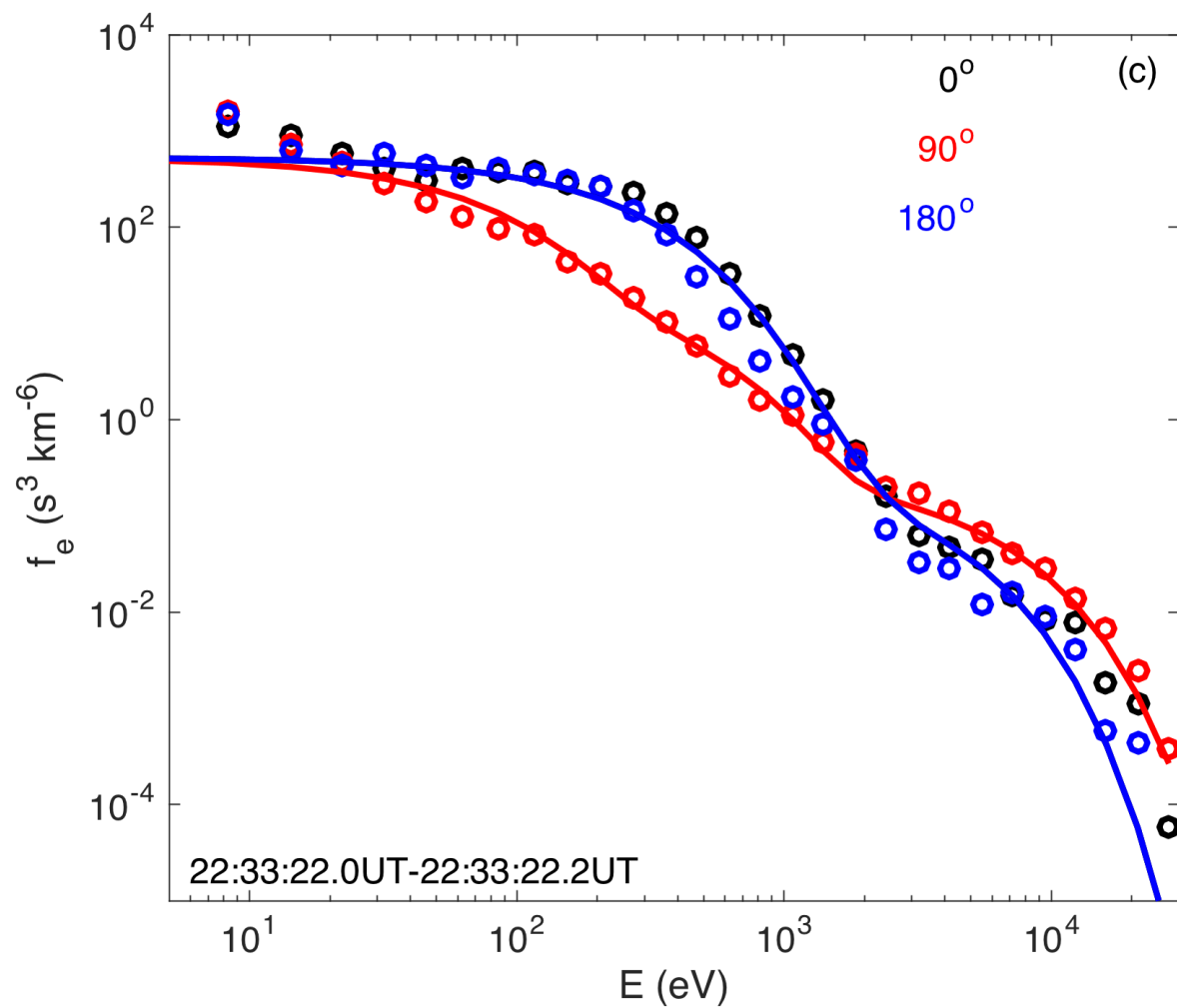
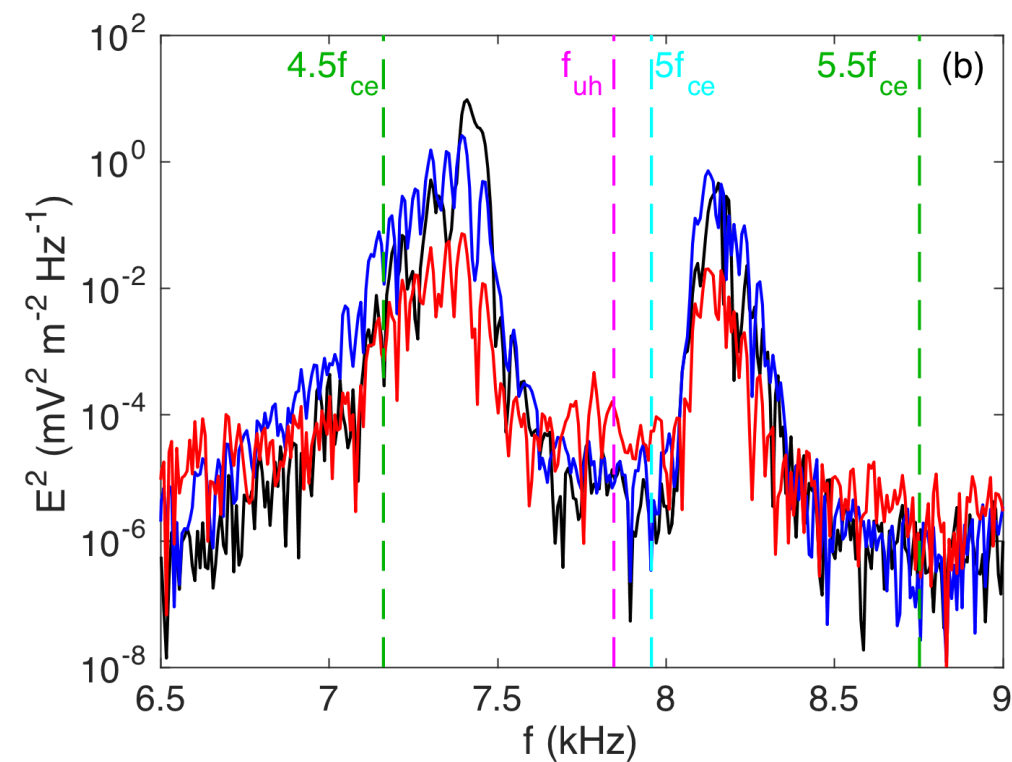
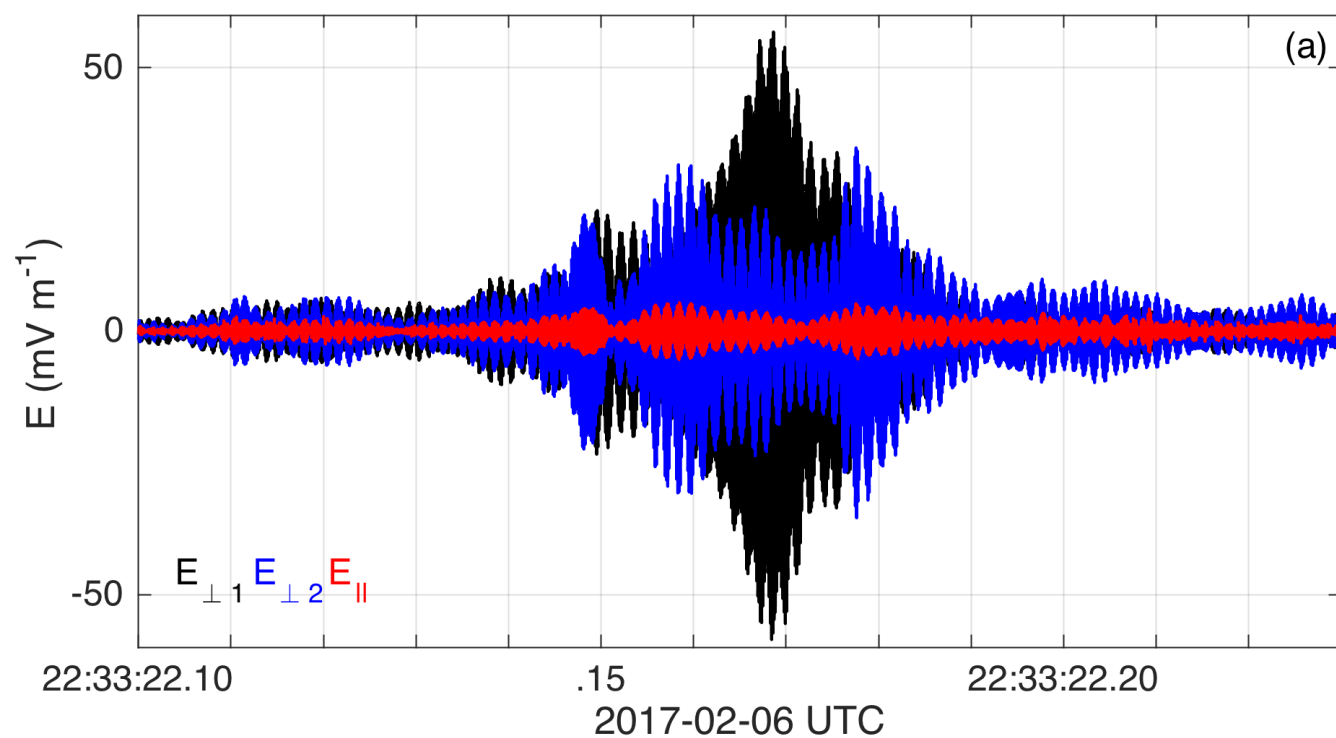
- Case 2 provides better agreement with observations.



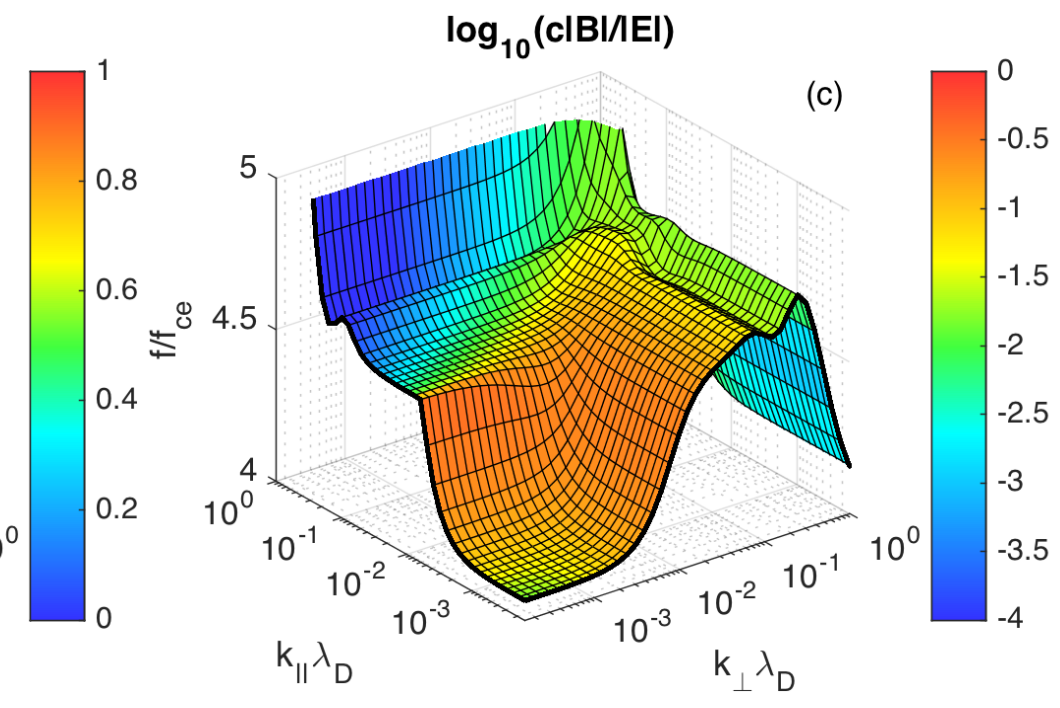
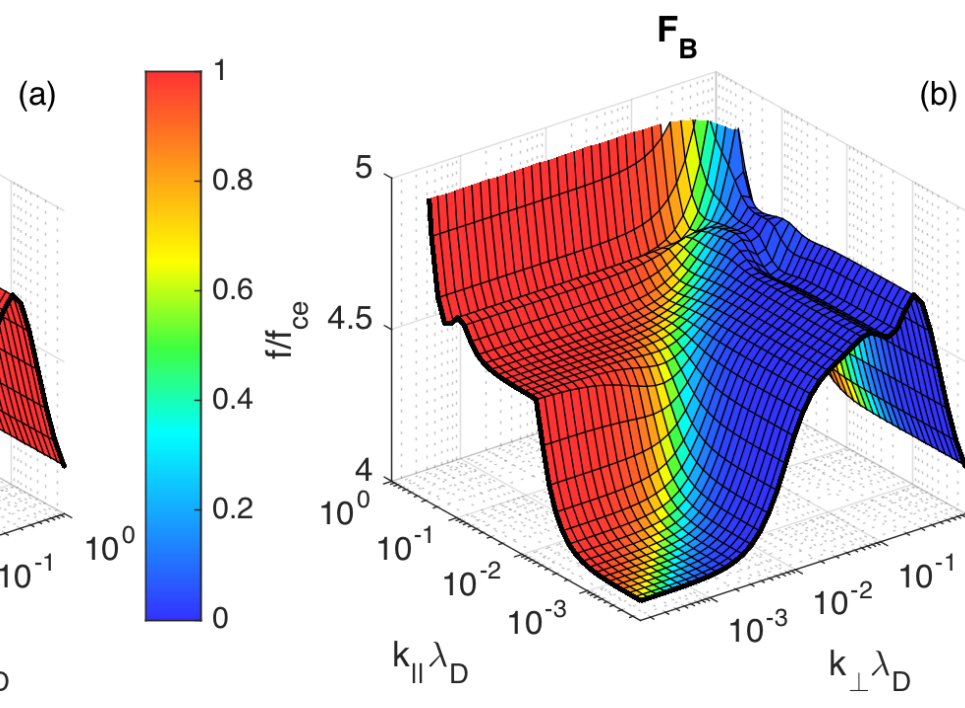
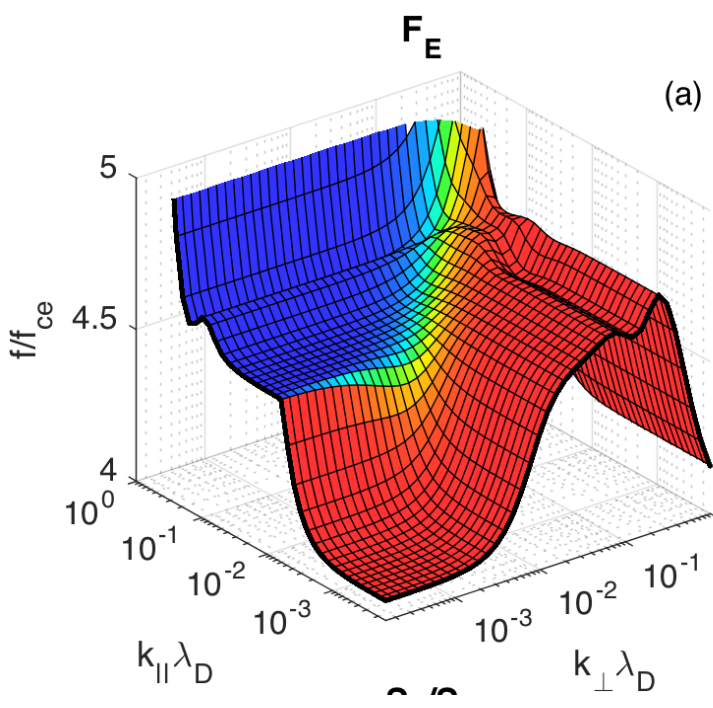
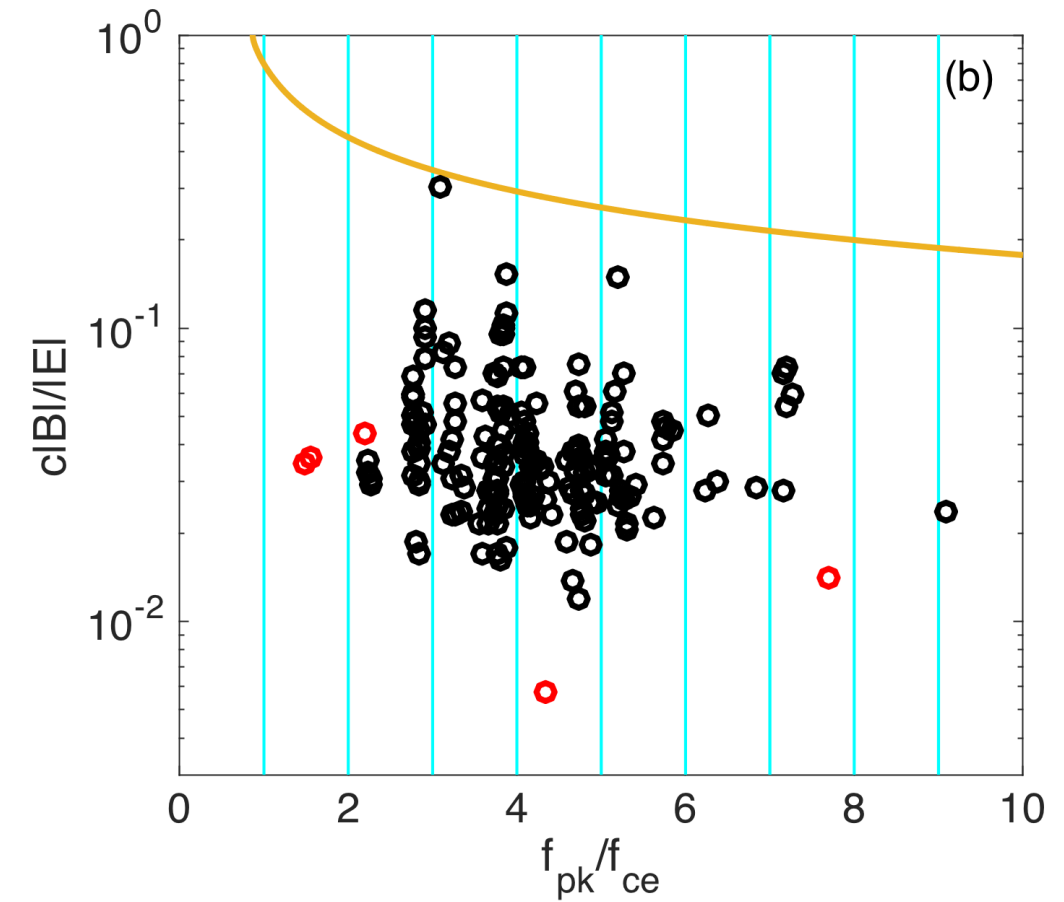
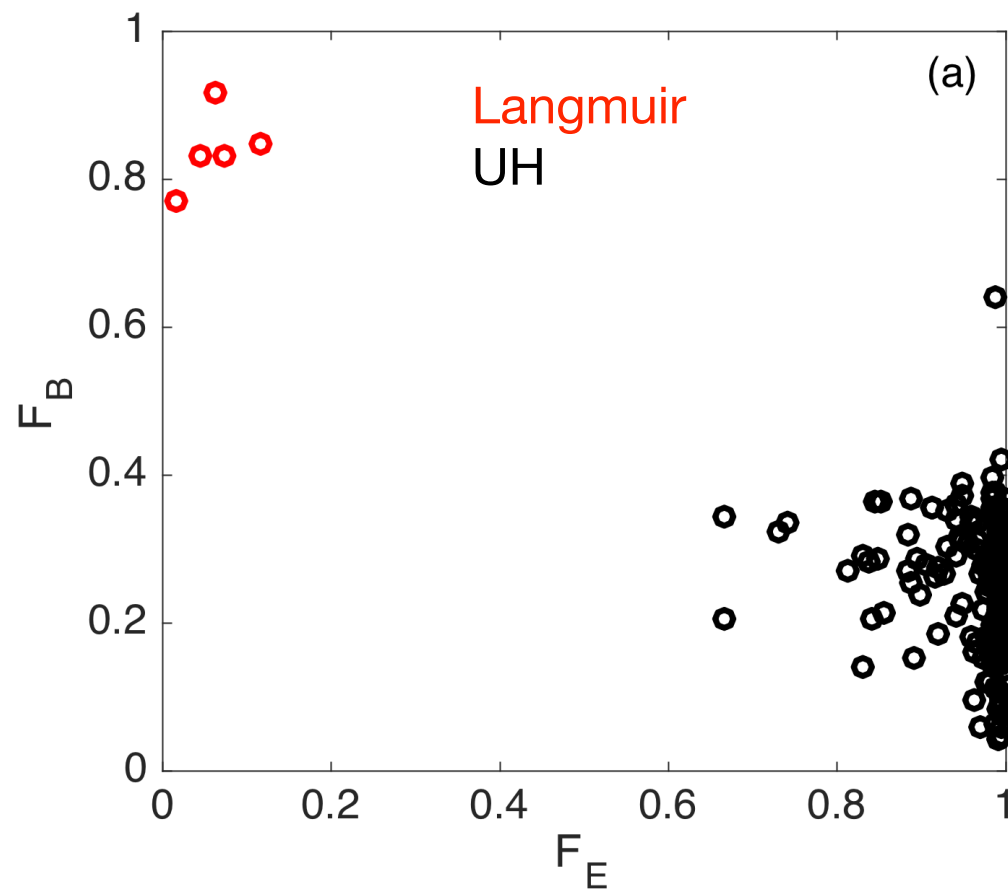
Example 1



Example 2



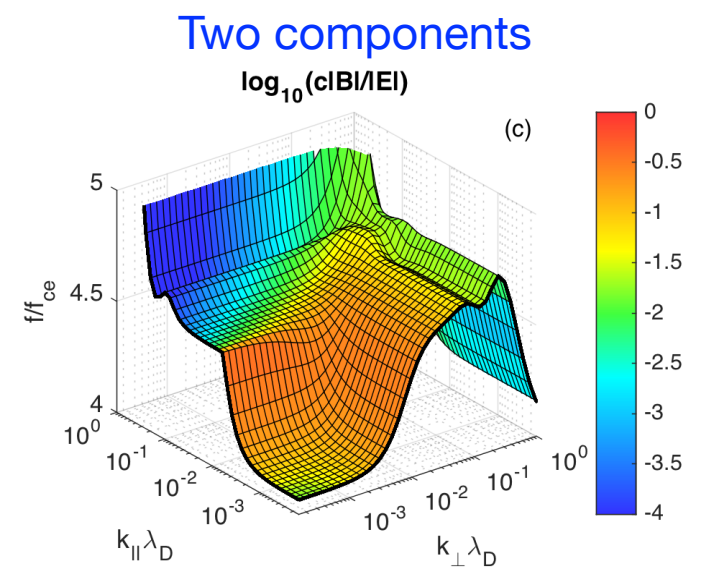
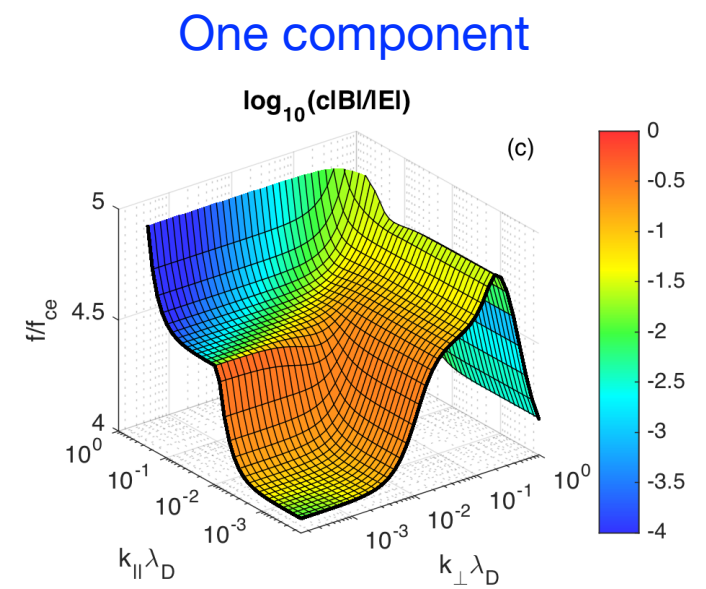
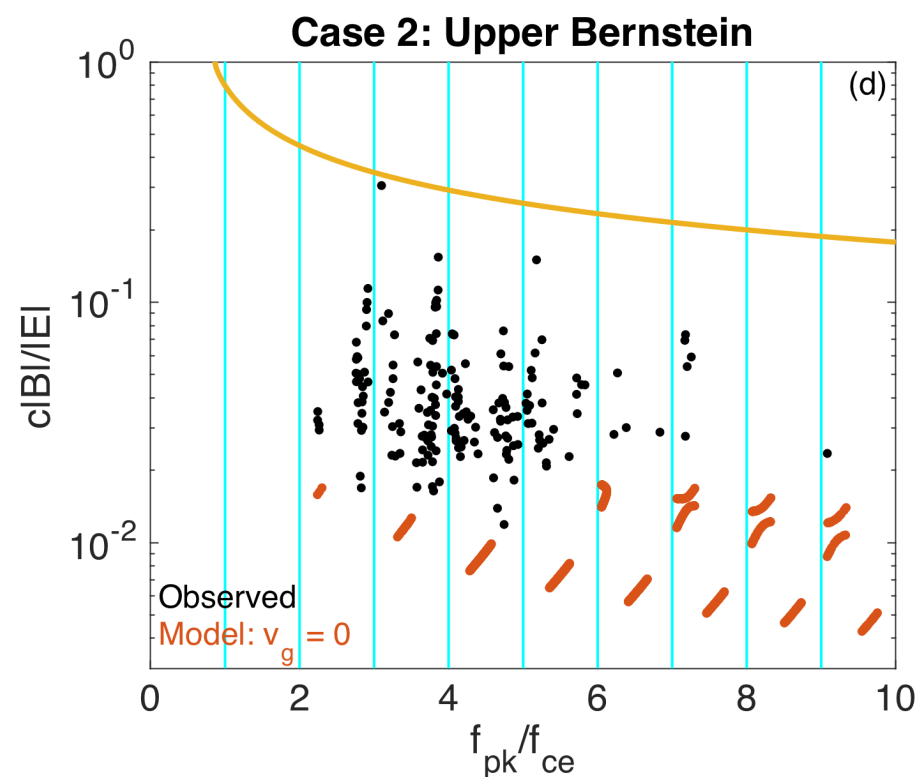
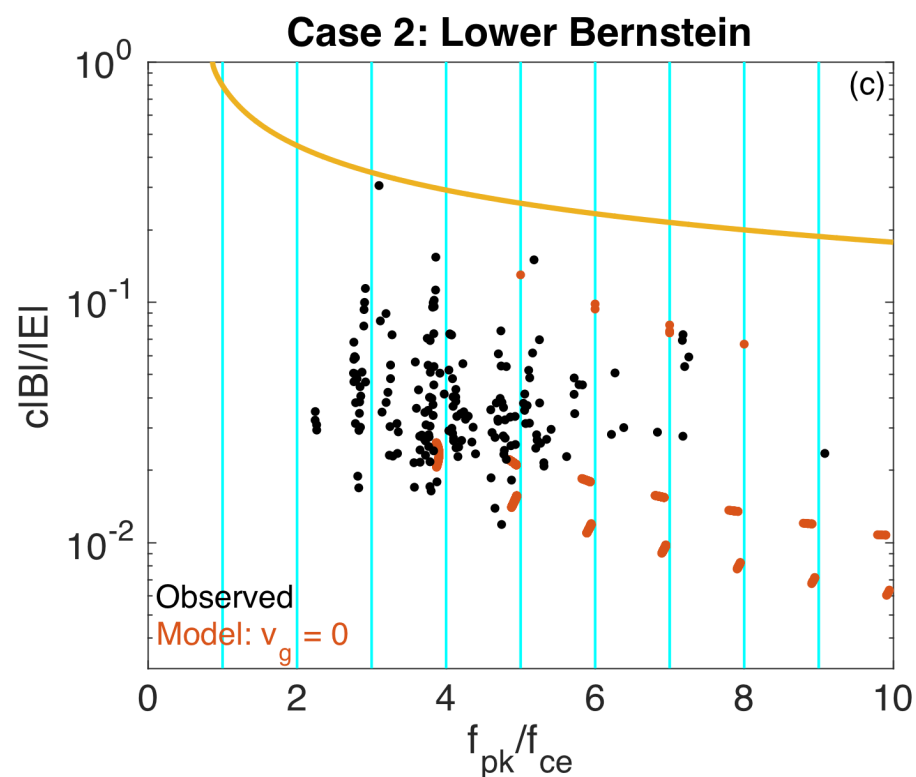
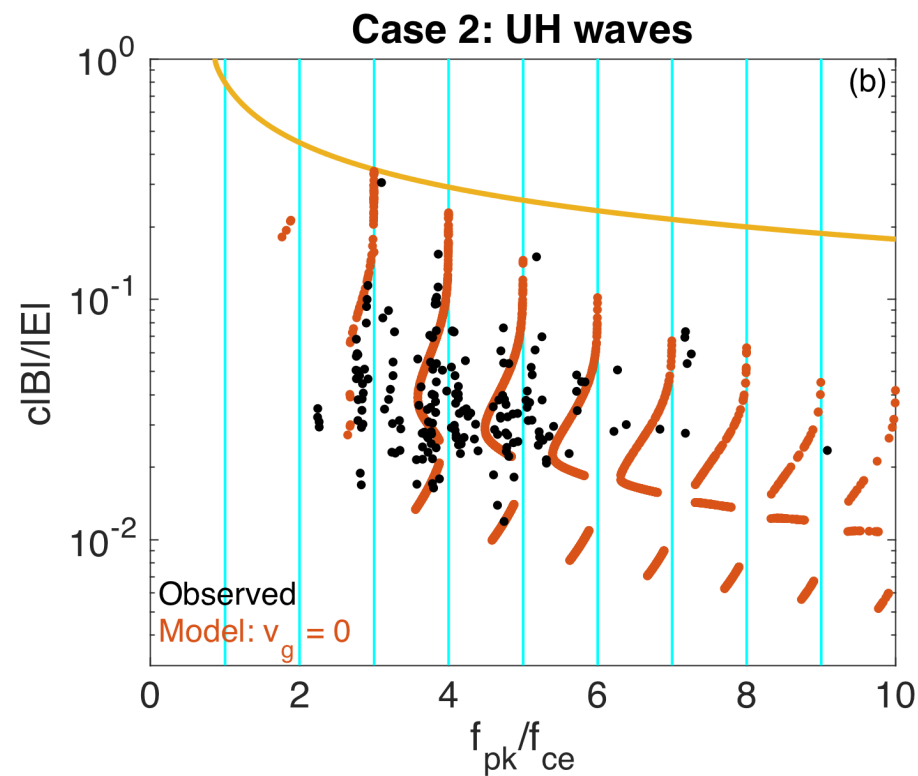
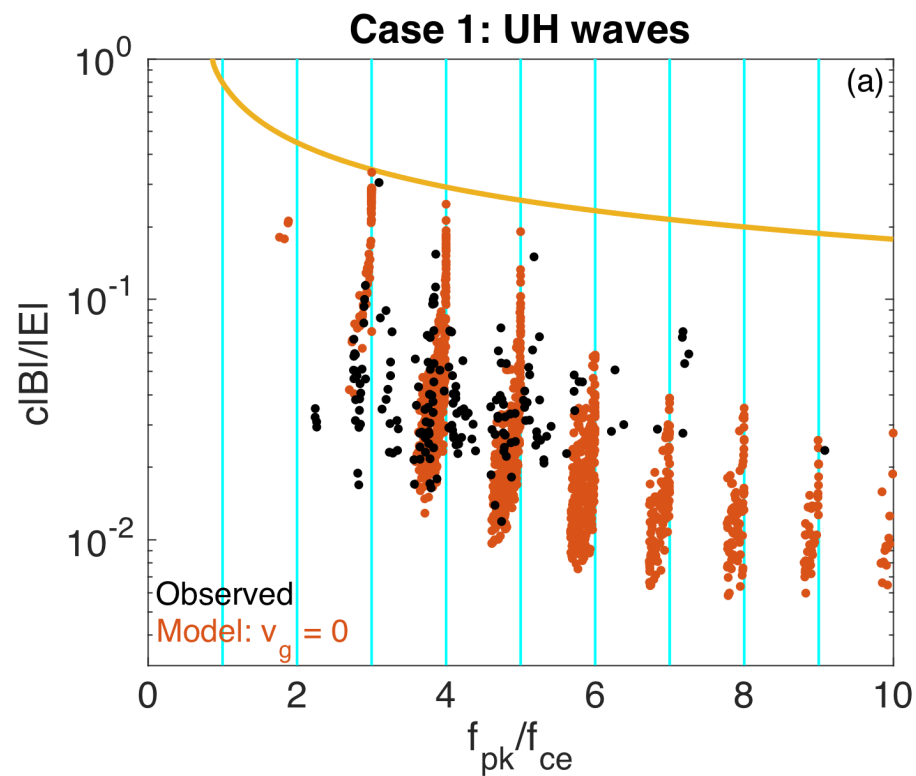
Electromagnetic properties



Comparison with kinetic theory

- Case 1: Single Maxwellian
- Case 2: Hot and Cold Maxwellians

- EM properties are consistent with UH waves rather than Bernstein waves.



Conclusions

- Large-amplitude Langmuir and UH waves are frequently observed at Earth's magnetopause.
- The electrostatic and electromagnetic properties of the waves are consistent with kinetic theory.